CHEMICAL REVIEWS

Review

pubs.acs.org/CR

Entangled Two-Dimensional Coordination Networks: A General Survey

Lucia Carlucci,*[,†] Gianfranco Ciani,[†] Davide M. Proserpio,*[,†,‡] Tatiana G. Mitina,[‡] and Vladislav A. Blatov*[,‡,§]

[†]Dipartimento di Chimica, Università degli Studi di Milano, Via C. Golgi 19, 20133 Milano, Italy

[‡]Samara Center for Theoretical Materials Science, Samara State University, Ac. Pavlov Street 1, Samara 443011, Russia

[§]Chemistry Department, Faculty of Science, King Abdulaziz University, Post Office Box 80203, Jeddah 21589, Saudi Arabia

S *Supporting Information*

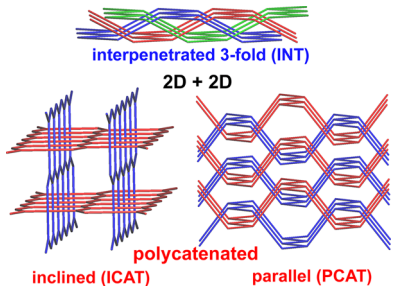

CONTENTS

1. INTRODUCTION

Many current investigations are focused on the design of new molecule-based functional materials. A great variety of extended architectures with promising properties has been obtained on the basis of crystal engineering concepts, both metal−organic and inorganic networks supported by coordinative/valence bonds and supramolecular arrays of organic and metal−organic molecules sustained by hydrogen bonds or other weak interactions.[1]

Many of the reported species exhibit the intriguing feature of interpenetration or other types of entanglements. The properties of these materials are related not only to their molecular structures but also to the topology of the individual networks as well as to the way in which the individual nets are entangled. It is therefore of basic relevance to analyze and classify these entanglements; in this concern, many contributions have appeared in recent years, dealing with rationalization of net interpenetration and elucidation of the different types of entangled systems.[2]

The extended species based on two-dimensional (2D) polymeric motifs (see Figure 1 for the evolution of reported 2D structures over the years) show particularly intriguing structures for many reasons: they exhibit a large variety of distinct topologies of single 2D nets and, in addition, show many different entanglement types, among which some puzzling cases were found that need a detailed discussion.[3] We must mention here the very complicated and intriguing case of the H-bonded network of trimesic acid, consisting of unusually polycatenated honeycomb (**hcb**) 2D layers, reported many years ago (1969).[4]

We have already reported our studies, based on the use of TOPOS (a package for multipurpose crystallochemical analysis),[7] on interpenetration in valence-bonded coordination[2d] and inorganic networks,[8] as well as in hydrogen-bonded supramolecular three-dimensional (3D) arrays formed by organic molecules[9] or by molecular complexes (zero-dimensional, 0D) and one- and two-dimensional (1D and 2D) coordination polymers.[10]

We report here the comprehensive results of our analysis of entanglements in coordination 2D networks from the Cambridge Structural Database (CSD, version 5.34, November 2012) using the latest version of TOPOS. Only valence-bonded 2D metal-based coordination networks are considered here, that can produce different types of entangled systems; supramolecular frameworks obtained by hydrogen bonds and/or other weak interactions like halogen bonds will be considered in future work. According to our previous investigations,[2c,e,f] we have observed that these different types can be classified as interpenetrated, polycatenated (parallel or inclined), or Borromean-linked arrays. Indeed, other subclasses have been evidenced and will be discussed below.

Received: March 14, 2014
Published: June 11, 2014

   dx.doi.org/10.1021/cr500150m | *Chem. Rev.* 2014, 114, 7557−7580

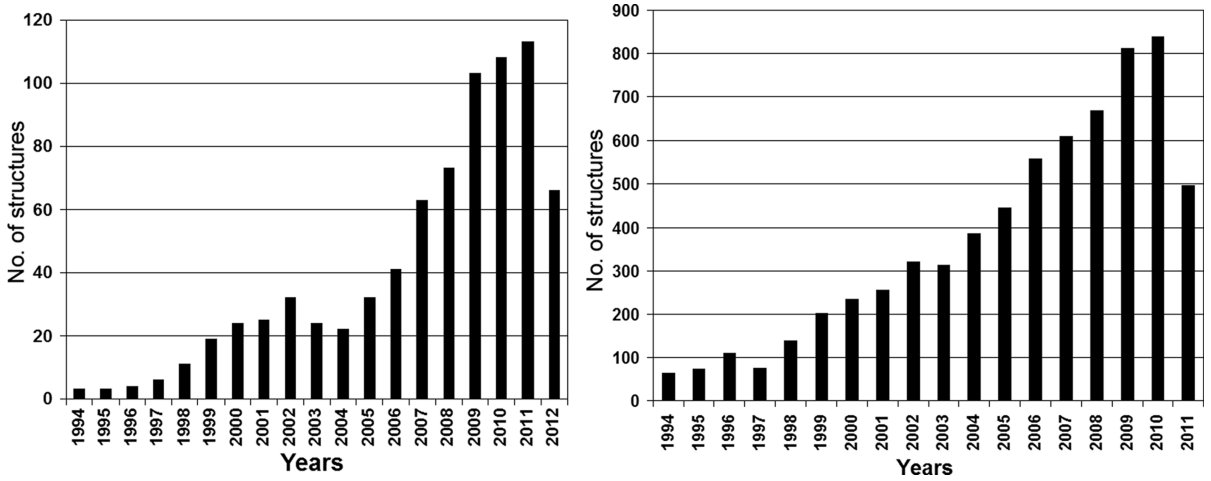

Figure 1. (Left) Distribution of 2D entangled coordination networks since 1994. The first example was reported in 1966 (not shown) with silver tricyanomethide, $AgC(CN)_3$ [AGMANI], giving a 2-fold interpenetrated **hcb** network, correctly described by Konnert and Britton.[5] (Right) Distribution of single (not entangled) 2D coordination networks since 1994 (data up to 2011 were taken from ref 3). The trends follow the explosion of interest of research into the realm of coordination networks and metal−organic frameworks (MOFs).[6] Note from the graphs that nonentangled species are about 8 times more frequent than entangled ones.

After this classification, we have also examined the potential functional applications of these entangled species in order to possibly establish a structure/properties relationship depending on the type of entanglement. Porosity has been one of the first recognized and investigated properties of coordination networks, and the search for robust and second-generation porous coordination networks has been strongly pursued, opening perspectives for real application of these crystalline materials in many technological fields. Easy tailoring of pore size and shape, as well as easy chemical functionalization of the networked structures, introduce features not characterized before for other porous materials. Flexibility/dynamism is one of these features and the main origin for network softness, a topic of increasing interest, addressed in the literature by many reviews and articles.[11] It is associated with the occurrence of a reversible structural change as a consequence of chemical or physical external stimuli such as interaction with guest molecules, pressure, temperature, light, and so on. This structural flexibility can be advantageously used to develop porous soft materials with increased guest selectivity to be used, for example, as sensors or in gas separation technologies. Entanglement can be exploited to develop tailored flexible materials. Reducing the accessible free space of a porous network was negatively considered for a long time, but recently it has regained a lot of interest. In fact, it can be used to increase network stability and to tailor the shape and size of pores, increasing guest adsorption selectivity; and moreover, the mutual displacement of entangled rigid or flexible motifs is one of the mechanisms at the origin of softness in coordination networks. In addition, interpenetration can affect the physical properties of the material, for example, magnetism.[12] Different synthetic procedures have been developed to attain a certain control of entanglement in coordination networks, and recently some reviews have appeared that are focused on factors governing the entanglements, having in mind their potential applications;[13] however, these analyses are mostly devoted to 3D networks thanks to the great wealth of data on interpenetration.[2d] On the other hand, information on entanglements in 2D species, showing a remarkable richness of types, is still much scattered in the literature (with the properties only occasionally investigated), and a general survey and rationalization of the phenomena is timely.

2. ANALYSIS OF CRYSTAL STRUCTURES BY TOPOS

All procedures on search, retrieval, and topological analysis of the crystal structures as well as their representation were performed with the program package TOPOS.[7] The following general algorithm was used, all steps of which are implemented as TOPOS procedures. These steps (I−VI) are described here in full detail, while the results are discussed starting in section 3.

(I) Interatomic bonds were determined by the method of intersecting sectors that we applied recently for 3D coordination networks.[2d,14] This method uses Voronoi polyhedra in addition to atomic radii to determine valence bonds; it is best suited for organic and coordination compounds. We considered only coordination compounds; bonds with participation of alkali or alkaline-earth metals (Na, K, Rb, Cs, Ca, Sr, and Ba), as well as all metal−metal bonds, were ignored.

(II) For all coordination networks, we determined their periodicity. The following TOPOS algorithm was applied: starting from any metal atom A of the network, all those translationally equivalent A^T atoms are searched that are connected to A by chains of bonds A-(L-A′-L)-A^T of any length (where L is a finite ligand of any complexity and A′ is an atom related to A by a nontranslational symmetry operation). The number of independent translations (0, 1, 2, or 3) that relate A and A^T atoms determines the network periodicity. At the next steps, we have treated only 2-periodic networks. In this review, we prefer to talk of 2D net as 2-periodic, with the distinction of 2-periodic 2D nets for the ones that have a projection on a plane without crossing edges and/or coincident vertices, hence topologically planar nets, and thick layers for the 2-periodic 3D nets that instead cannot be projected on a plane without crossing edges and/or coincident vertices.

(III) All 2D networks were tested for the existence of entanglements. We assumed that the topological entanglement existed if at least one Hopf link or a multilink occurred between different 2D motifs. Separately, we searched for Borromean and Brunnian entanglements in which only non-Hopf interweaving existed within each group of *N* networks but all *N* networks

dx.doi.org/10.1021/cr500150m | *Chem. Rev.* 2014, 114, 7557−7580

formed a tightened interlacing array, with $N = 3$ for 2D Borromean and $N > 3$ for both 2D and 3D Borromean or Brunnian types of entanglement. All entangled arrays found were further analyzed at the next steps.

(IV) The following parameters of entanglement were determined: (a) entanglement type (interpenetration, inclined or parallel polycatenation, Borromean or Brunnian entanglement); (b) number of entangled nets in the interpenetrated array (Z); (c) degree of catenation (Doc)[2c] for inclined or parallel polycatenation, implying evaluation of the number of links (Hopf or multilink) a particular ring of one net forms with rings of other nets in the array; (d) index of separation (Is)[2c] of 2D motifs in the case of parallel polycatenation, that is, the number of motifs which have to be removed to disjoin the array into two separate parts; and (e) existence of 2-loops, that is, rings in which all nodes, but two, have coordination 2.

(V) All the networks were then simplified to obtain the underlying nets, that is, nets of centroids of structural groups. We have treated two types of simplification: the cluster one, where some structural groups were polynuclear complexes, and the standard one, where all metal atoms and ligands were regarded as nodes of the underlying net. If the underlying net contained 1- or 2-coordinated nodes (terminal or bridge structural groups), it was simplified further by removing the terminal nodes and replacing the bridge nodes by net edges. Simplification of a network that contains 2-loops can lead to complete disappearance of the entanglement, and therefore such networks were picked out into a separate group.[14] We decided to report only one type of underlying net for each structure; in particular, a cluster description was used when structural building units were evident (e.g., paddle wheels, dimers, etc.)[15]

(VI) The overall topologies of underlying nets were determined with the TOPOS TTD collection, which currently contains more than 75 000 net topologies. To designate the topologies we have used three nomenclatures: Reticular Chemistry Structure Resource (RCSR) three-letter symbols,[16] which were introduced for the simplest plane nets; Fischer and Koch's symbols for 2D packing of spheres;[17] and TOPOS *ND*k symbols,[14] which are used in the TOPOS TTD collection for those topologies that are not covered by the first two nomenclatures.

3. TOPOLOGIES AND ENTANGLEMENTS OF TWO-DIMENSIONAL COORDINATION MOTIFS

The results of our investigation have revealed that there are 783 2D motifs that form entangled arrays, representing ca. 7% of the total number of the structurally characterized 2D species.[3] We have, at first, analyzed the topologies of individual 2D motifs forming the entangled arrays and we found 36 distinct nets (all illustrated in Figures 3, 4, and 11 and Figure S1 in Supporting Information). The distribution of network topologies appearing at least two times (13 out of the 36 distinct topologies overall observed) is illustrated in Figure 2. Among the 36 different network topologies found within all 783 analyzed structures, **sql** is the most common, with 465 cases, and **hcb** is second, with 206 cases. The remaining 112 structures show 34 different topologies, and 23 of these are represented by a single structure. Nine of the 36 characterized topologies are intrinsically planar 2-periodic 2D (their projection does not have any edge crossings) and account for 90% of all structures (706/783) (Figure 3); all nine topologies have been observed also not entangled.[3] The 27 remaining topologies are thick layers or multilayers (2-periodic 3D) and refer to 77 structures, 65 of which are parallel

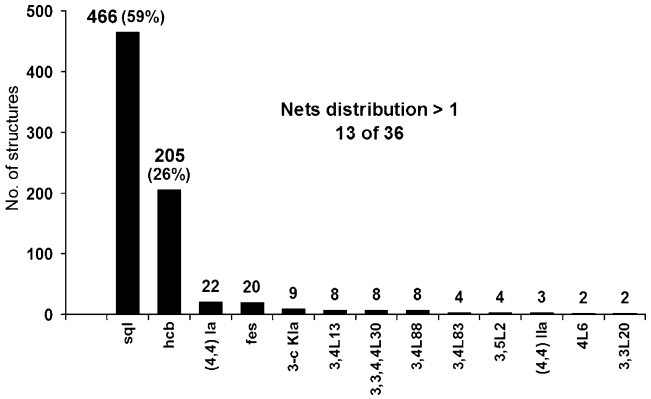

Figure 2. Net distribution of the 783 2D entangled motifs.

polycatenated (PCAT) with 20 different topologies, eight interpenetrated (INT), one inclined polycatenated (ICAT), and three with mixed types of entanglement. The different types of entanglement described here were introduced some years ago;[2c,e,f] they are discussed in detail below.

A comparison of single[3] versus entangled 2D nets shows that **sql** and **hcb** are the most frequent in both cases; moreover, 10 entangled nets among the first 11 observed (>2) (listed in Figure 2) are also found among the first 14 most frequent single 2D nets.

Ten thick-layer nets, including 3,3,4,4L30 (eight occurrences) and nine other topologies (with one occurrence each), are observed exclusively within entangled species (see Figures 4 and 11). The remaining 17 thick layers, observed also in non-entangled species, are reported in Figure S1 in Supporting Information.

Within the thick layers the 3-c (8^2.10)-KIa net (see Figure 5) is peculiar since it shows the uncommon phenomenon of different realization of the same graph in space (embeddings) that cannot be deformed into each other without breaking edges; this property is called "non-ambient isotopy".[2e,h] We observed here and also in the analysis of nonentangled cases (in detail: seven PCAT, two INT, and 69 nonentangled structures) three different nonambient isotopic embeddings of (8^2.10)-KIa net, as illustrated in Figure 5. All the statistics illustrated above can be checked in detail with the data available as Supporting Information

Two planar nets that rank in the top 10 list of most frequent single 2D layers do not give entanglement: 3^6-**hxl** (hexagonal lattice), likely due to the presence of the smallest 3-rings and 4,4L1, which arises from the standard representation of the numerous paddle-wheel decorated **sql** nets. In this work, we choose to give only one representation for each compound, hence 4,4L1 nets are here reported as **sql** (see Figure S2 in Supporting Information). Instead, the fourth most frequent type (with 485 structures reported in ref 3) of single 2D nets, the (3,6)-c **kgd** net, has been observed only in one structure, $Zn_5(bpib)_2(L)_4(OH)_2(H_2O)_2$ {TONFUY, where bpib =1,4-bis[2-(pyridin-2-yl)-1*H*-imidazol-1-yl]butane and H_2L= 3,3′-methylenebis(oxy)dibenzoic acid}[18] as 2-fold interpenetrated. The rhombic geometry of **kgd** makes it less flexible, hampering entanglement; only the presence of bent ligands supports this topology in TONFUY (see Figure S3 in Supporting Information). Other topologies observed in not entangled 2D nets[3] are probably less suited to give interlaced species.

To include all the phenomena observed here, we extend the definition of entanglement introduced some years ago:[2c,f] together with the classical interpenetration and polycatenation

dx.doi.org/10.1021/cr500150m | *Chem. Rev.* 2014, 114, 7557−7580

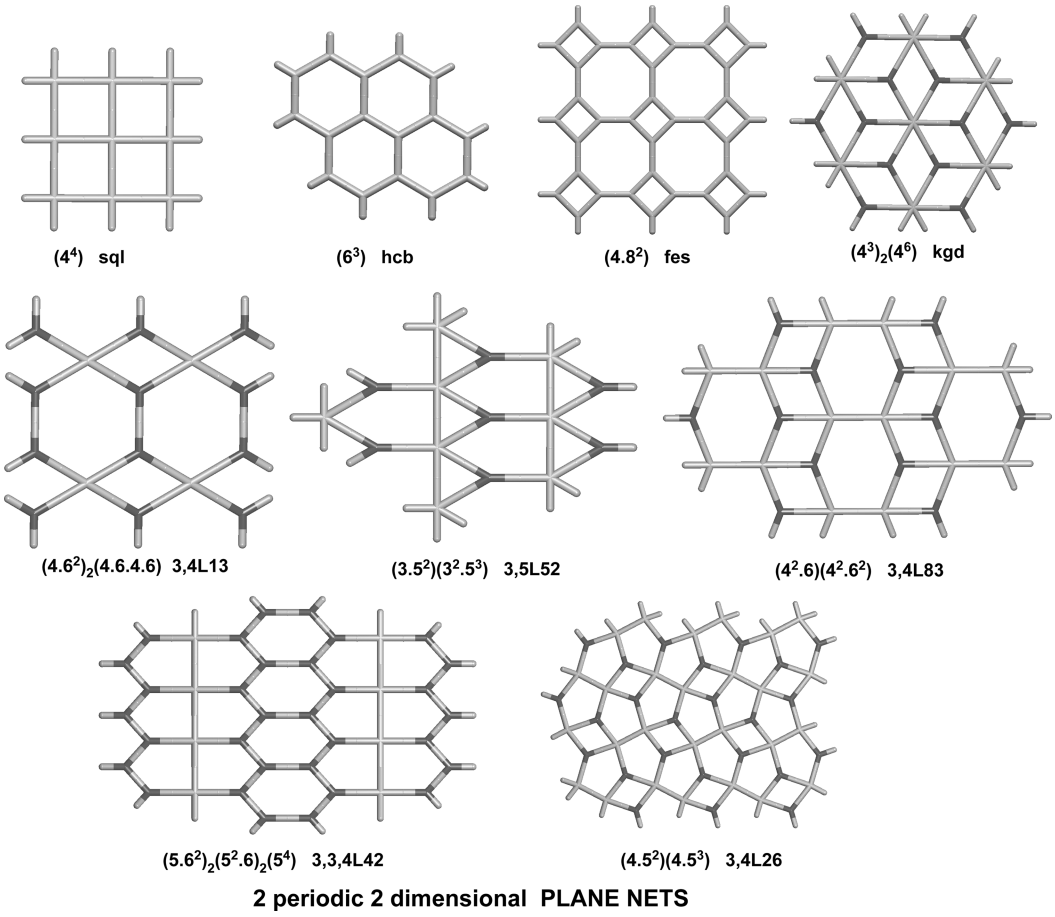

Figure 3. Nine observed planar nets (2-periodic 2D).

(parallel and inclined) via Hopf links, we observed many examples of entangled 2D nets with 2-loops via rotaxane links.[19] A scheme that includes all possible observed and not-yet-observed cases is given in Figure 6. The main distinction illustrated here is between interpenetration (INT, left column) and polycatenation (parallel PCAT or inclined ICAT, right column). These two basic types of entanglement show quite distinct topological features that are listed in the two columns. Within polycatenation the distinct layers can interlace via Hopf links either in parallel fashion (all layers are parallel) or in inclined fashion (two or more sets of parallel layers forming a certain nonzero angle); this difference was evidenced since the 1990s and was widely discussed in the review by Batten and Robson.[2a] In total, there are 345 interpenetrated (INT), 127 polycatenated parallel (PCAT), and 222 inclined (ICAT) coordination networks. The remaining structures (not included in the above scheme) comprise 31 Borromean entangled (BORR),[20] 15 species (MIXED) that cannot be strictly assigned to any of the previous classes showing mixed type of entanglement, and 43 structures containing 2-loop rings (of these, there are 39 INT, two PCAT, and two ICAT). The pie chart illustrated in Figure 7 shows an almost equal distribution of interpenetration (345 + 39 = 384) and polycatenation (127 + 222 + 2 + 2 = 353), with only 5.9% different phenomena (MIXED + BORR). Polyrotaxane entanglement via 2-loops is also represented by a small sample (5.5%). The 77 structures (10% of the whole sample) that are represented by thick layers have mostly polycatenated parallel entanglement (84%), showing that the nonplanarity of a layer favors parallel entanglement.

3.1. Interpenetration

Interpenetrated 2D layers represent the most numerous group (overall 384 entries). This type of entanglement is generally characterized by the presence of 2D identical motifs that are interlaced, sharing the same average plane. The degree of interpenetration Z is equal to the total number of such motifs. We have previously investigated the interpenetration of 3D coordination networks and have suggested a classification related to the distinct modes in which individual identical motifs can interpenetrate, represented by the operations that generate the whole array from a single net (classes I, II, and III).[2d,8] Though this approach has a potential heuristic validity and has been usefully applied in the analysis of interpenetration in many 3D systems,[2d,14] it is essentially based on geometrical, rather than topological, criteria since it describes interpenetration simply in terms of crystallographic symmetry relations (we may call them "crystal classes of interpenetration"). Taking into account the growing tendency to focus interest on true topological descriptions of the entangled networks, as evidenced by recent investigations and new approaches,[21] we have decided to neglect here this classification.

The maximum value observed for Z is 6, found only in **hcb** [Ag(1,3,5-tris(4-ethynylbenzonitrile)benzene)CF_3SO_3]·2C_6H_6 (ZABQIC01;[22] see Figure 8) reported in 1996, well below the exceptional records found in a recently reported 3D metal–organic 10^3-**srs** network (54-fold, OYEYOH)[23] and also in a 3D organic H-bonded 10^3-**srs** network (18-fold, SAYMUB01).[24]

dx.doi.org/10.1021/cr500150m | Chem. Rev. 2014, 114, 7557–7580

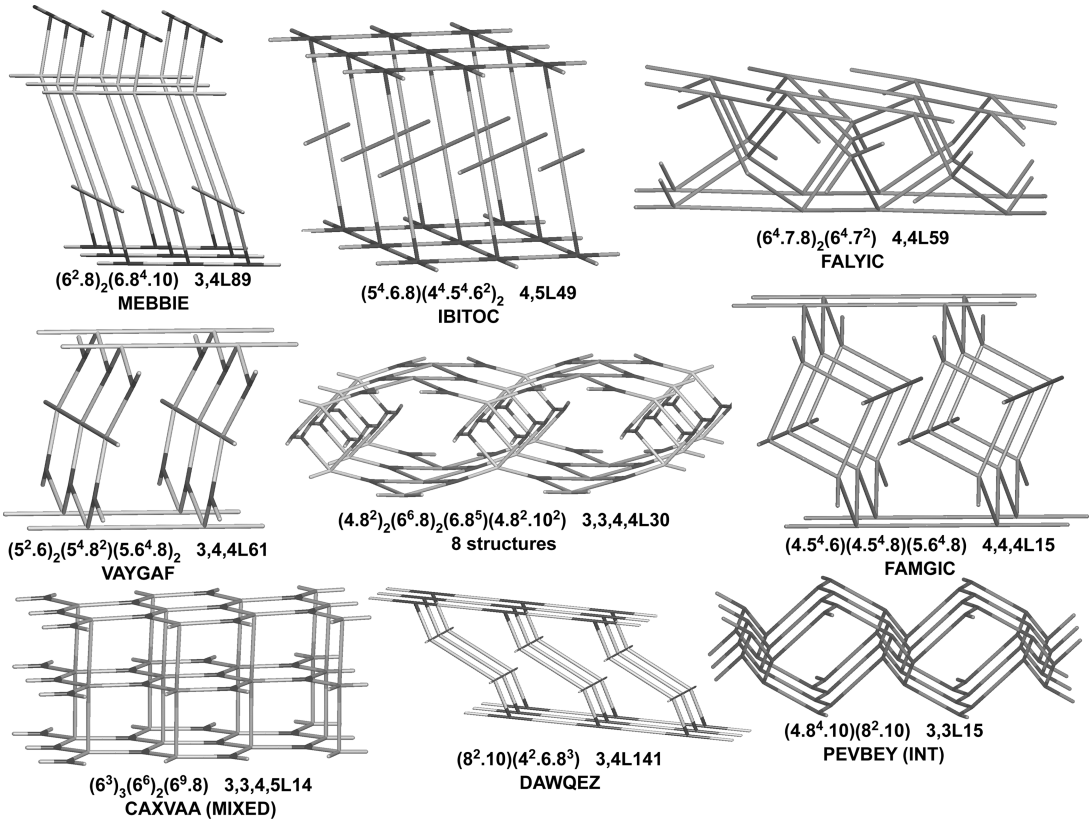

Figure 4. Nine new topologies observed only within entangled 2D nets; seven are observed within parallel polycatenation (PCAT), one within mixed type (bottom left), and one within interpenetration (INT). Refcodes for the nets observed in only one structure are given.

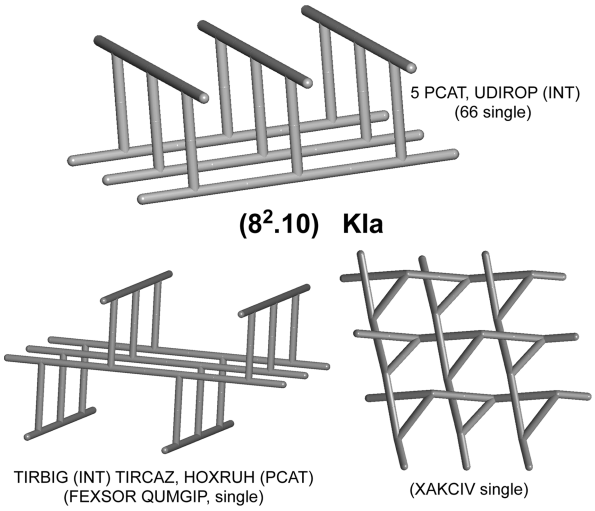

Figure 5. Three different (non-ambient isotopic) embeddings of KIa observed in 2D structures (nine entangled and 69 single) that cannot be deformed into each other without crossing edges.

High values of Z are rare (only three 5-fold and seven 4-fold cases) and the large majority of examples are 2-fold interpenetrated (>79%).

We must mention here an interesting case that describes a unique linking mode between the rings of interpenetrating motifs in polymeric networks. In most cases, the shortest circuits of individual pairs of networks catenate only with 2-crossing [2]-catenane motifs, equivalent to the 2-component link with 2-crossing, the Hopf link. However, in six 2-fold interpenetrated structures with topology **sql**, the 4-crossing [2]-catenane motif (equivalent to the 2-component link with 4-crossings called Solomon link/knot) has been found: [M(dde)(bpp)]·H_2O [where dde = 4,4′-dicarboxydiphenyl ether and bpp = 1,3-bis(4-pyridyl)propane], with M = Cu (COKPIC),[25] Ni (COKPOI),[25] or Co (SOCYEP,[26] SOCYEP01[25]), and M(bbmb)$_2$(Cl)(OH)]-(H_2O)$_2$ [where bbmb = 4,4′-bis(benzimidazol-1-ylmethyl)-biphenyl], with M = Ni (FUYWIG)[27] and Cu (FUYWOM)[27] (see Figure 9). Such multicrossing links are rarely observed also in 3D interpenetration; one known example is the 4-crossing [2]-catenane motif identified for 2-fold quartz **qtz** nets.[28]

An analysis of the 2D interpenetrating nets listed by TOPOS shows the presence of subgroups of structures having peculiar geometrical and topological features that make them well distinct from the remainder. One subgroup comprises species with layers containing 2-node loops (2-membered rings) that are threaded by spacers forming edges of the 2D layers (39 entries in the list). This subgroup (we can call this type of entanglement "polythreaded interpenetration") has been the subject of a recent review[19] and will be discussed in more detail in section 3.2.

In the second subgroup, comprising, at present, only a few species, the interlaced layers are not coplanar but show a relative displacement in the stacking direction. By extrapolation from the few real cases, we can imagine an entire new class of networks that can be considered as cuts of 3D parallel polycatenated arrays (like the three interlaced nets in Figure 10), with a finite number n of catenated layers (n-catenation). While interpenetration of layers implies that each motif is interlaced with all the other ones of the array, this is not the case for the first species in Figure 10, where the average planes of adjacent layers are displaced along the stacking direction: this example at present has never been observed.

dx.doi.org/10.1021/cr500150m | *Chem. Rev.* 2014, 114, 7557−7580

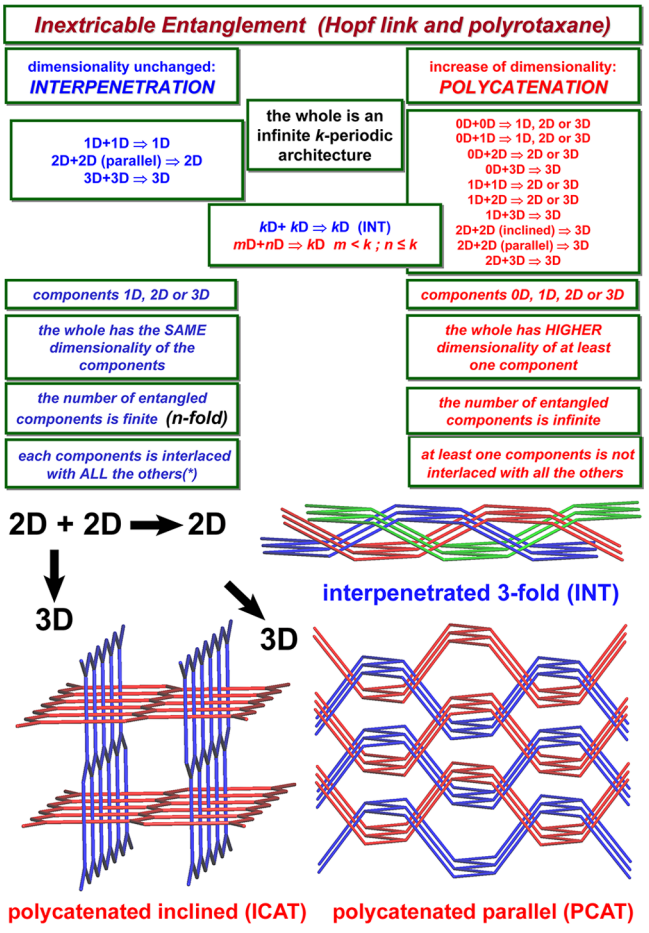

Figure 6. (Top) Complete scheme of classification of entanglement in periodic structures. (*) This condition is disregarded for only one structure, EWOTAM; see text. (Bottom) Examples of entanglement of **hcb** nets showing the difference between interpenetration and polycatenation (parallel and inclined).

We can include in this new family $[Cd_2(bpt)(ip)_2(H_2O)_4]\cdot 6H_2O$ [where bpt = 4-amino-3,5-bis(4-pyridyl)-1,2,4-triazole and ip = isophthalate] (UDIROP)[29] and $\{[Cd_2(TPOM)(hfipbb)_2]$ [where TPOM = tetrakis(4-pyridyloxy-methylene)-methane and H_2fipbb = 4,4′-(hexafluoroisopropylidene)bis-(benzoic acid)] (FAMGEH)[30] (see Figure 10) that are both 2-catenated arrays.

Another example is $[Co_2(bipe)_{1.5}(bta)(H_2O)_4][Co(bipe)(bta)](H_2O)_{0.5}$ [where H_3bta = benzene-1,2,3-tricarboxylic acid and bipe =1,2-bis(4-pyridyl)ethane] (EWOTAM)[31] (see Figure 11), a 3-catenated array in which a 3,3,3L5 complex unique central self-catenated layer (shown in blue in Figure 11) is

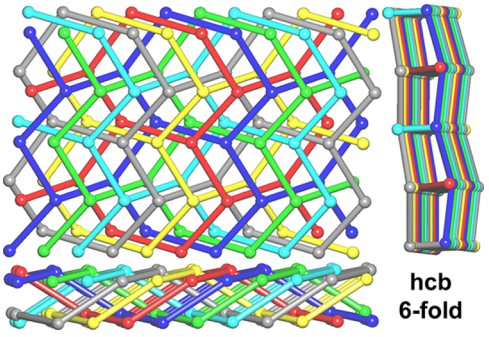

Figure 8. Maximum interpenetration observed in 6-fold **hcb** [Ag(1,3,5-tris(4-ethynylbenzonitrile)benzene)CF_3SO_3]·2C_6H_6 (ZABQIC01).

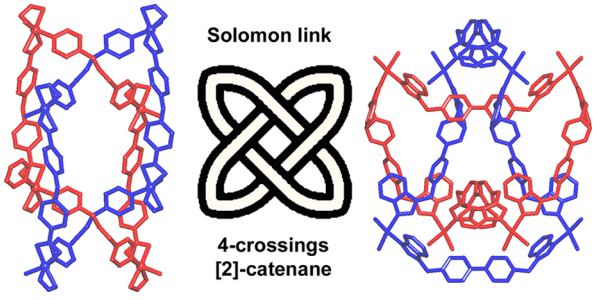

Figure 9. Rare case of 2-component link with 4-crossings observed in six 2-fold interpenetrated **sql** structures: (left) $[M(dde)(bpp)]\cdot H_2O$ and (right) $M(bbmb)_2(Cl)(OH)](H_2O)_2$ (see text).[25−27]

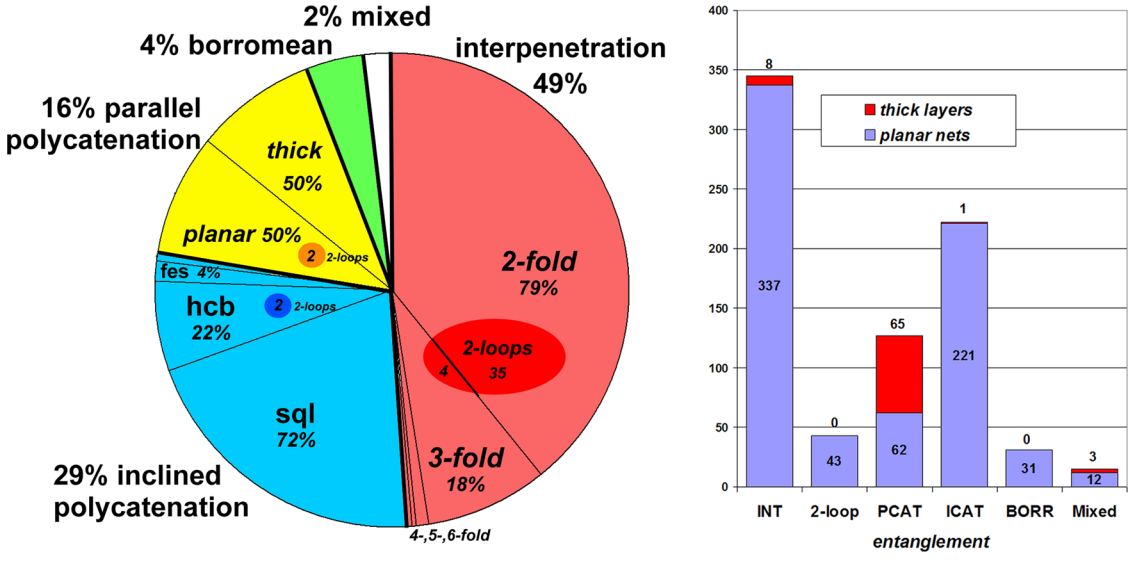

Figure 7. (Left) Distribution of interpenetration vs polycatenation in 783 2D entangled structures. (Right) Distribution of thick and planar layers among the six types of entangled structures.

dx.doi.org/10.1021/cr500150m | Chem. Rev. 2014, 114, 7557−7580

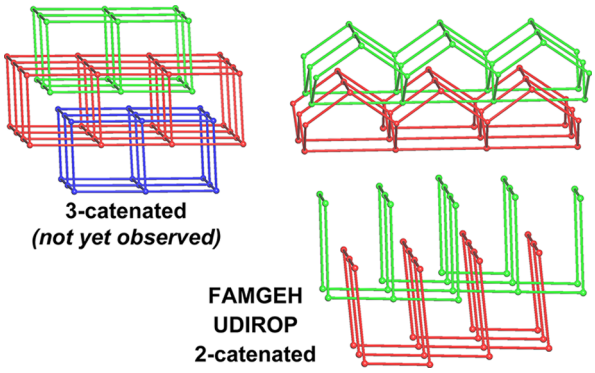

Figure 10. Possible interpenetration with the equivalent interlaced layers not coplanar but with a relative displacement in the stacking direction. Only the 2-fold 2-catenated motif has been observed.

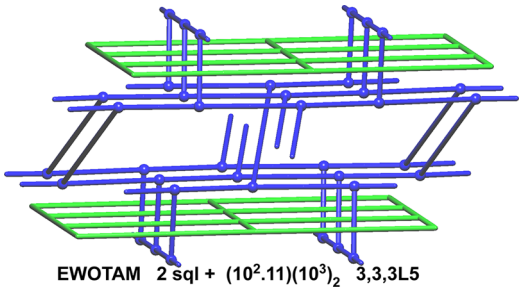

Figure 11. Unique 3-catenated array with nonequivalent layers observed in EWOTAM.

interlaced with two equal upper and lower **sql** layers (shown in green in Figure 11). It is not possible to speak here of true interpenetration since the layers are different and the external two are not interlinked.

The difficulties in the study of entanglements can produce wrong descriptions in the literature: for example, in the structure of $Zn_3(BIDPE)_3(5\text{-}HIPA)_3{\cdot}4H_2O$ [where BIDPE = 4,4′-bis-(imidazol-1-yl)diphenyl ether and 5-HIPA = 5-hydroxyisophthalate] (IXOHOT),[32] the authors describe this species as a case of "finite polycatenation", consisting of six catenated **sql** layers. Unfortunately, their claim that "this is the first report of six identical sheets polycatenated still to form a 2D → 2D network" is wrong; the more usual 2D → 3D parallel polycatenation is observed here, according to analysis with TOPOS.

When the three above *n*-catenated (not truly interpenetrated) species are neglected, all other cases of true interpenetration are composed of identical coplanar motifs except for two examples, ($[Mn(NCS)_2(4,4'\text{-bis-pyridylpropane})_2]{\cdot}0.25H_2O$; MULFEE[33] and REDSEZ[34]), where the two interpenetrating layers are very similar but crystallographically independent with small differences in conformations of the flexible ligands. The occurrence of different interlaced 2D motifs, on the other hand, is much more frequent in other types of entanglements, such as inclined polycatenation (see section 3.4).

Interpenetration of **sql** layers supports solid-state reactions via single-crystal to single-crystal (SCSC) transformation, from 4-fold **sql** to 4-fold **dia**[35] and guest-driven ligand exchange.[36] We can mention here also the nonlinear optics (NLO) properties with strong second harmonic generation (SHG) effect of a 2-fold interpenetrated **sql** species.[37]

3.2. Entanglements of Two-Dimensional Layers Containing 2-Membered Loops

A closer examination of the list of interpenetrating 2D networks obtained from TOPOS reveals the presence of a significant number of cases with layers containing 2-membered rings. They form a special subclass within interpenetration (we suggest the name "polythreaded interpenetration"), with the peculiar feature that the entanglement consists of threading of the 2-node loops by edges of adjacent layers (Table 1).

If one applies the normal simplification process used in the network approach for topological classification of the layer, the risk is to overview the entanglement. Indeed, there are many 1D, 2D, and 3D frameworks containing 2-node rings that are not topologically significant, but this is not true in the present species. As clearly discussed for the first time by Ma, Batten, and co-workers,[38] here the 2-node loops must be explicitly considered. A special topological notation is required for the single layer: a vertex symbol (VS) that includes also the 2-connected nodes is suggested instead of the usual VS of the underlying simplified 2D net, and this special notation has been added into TOPOS. These entangled species can be described as polyrotaxane-like structures and were previously included in the cases of polythreading.[2c] Two "older" examples shown in Figure 12 have been known since the mid-1990s, but since 2007 many new fascinating species of this type have been reported.

During preparation of this paper, a review[19] has appeared describing in detail these species containing 2-membered loops, with interesting comments. The concept of "nontrivial polyrotaxane" is introduced and a definition is proposed.[19,39] We will use when possible (in Table 1) the classification illustrated by these authors.

All these species are formed by the interlacing of layers of four distinct topological types only, illustrated in Figure 13, whose simplified topologies are **hcb** (2,4L1) and **sql** for 2,6L1, 2,6L2, and 2,10L1, which differ in the position and number of the 2-node loops.

Inextricable entanglements of these layers exhibit the presence of rotaxane-like linkages of different types, depending on the number of rods and rings involved. By analogy with the classification suggested for molecular rotaxanes,[69] we can adopt when possible a notation like the following one: 1.1 (one rod, one ring), 1.2 (one rod, two rings), 2.1 (two rods, one ring), 2.2 (two rods, two rings) and so on.

The cases of 2-fold interpenetration (35 entries out of 43, the large majority in Table 1) are almost equally distributed between the two structures I and II shown above in Figure 12 (classified as IIIa and IIIb, respectively, in ref 19). In these species, the usual links are rotaxanes of type 1.1.

There are only three recent exceptions (DAYMEX,[41] ETEKUK,[43] and UYOHOG;[61] see Figure 14); these contain the layers 2,10L1 with peculiar structural features such that rods of the second layer are threaded by two adjacent loops of the first layer and vice versa. Thus, the rotaxane links are of type 1.2.

It is worth mentioning here that there is only one species, at present, containing layers of type 2,6L2: the 2-fold interpenetrated QUQGOZ[56] (type 1.1 rotaxane, see Figure 15). The examples of 3-fold interpenetration include two species with 2,4L1-type layers (WAGXAF and WAGXEJ)[66] and two with 2,6L1 type layers (NUDDEW[54] and TONGAF[60]), illustrated in Figure 15). In the two former cases, each loop is threaded by two rods and each rod threads only one ring (rotaxane type 2.1), while in the latter two cases each loop is threaded by two rods and

dx.doi.org/10.1021/cr500150m | Chem. Rev. 2014, 114, 7557−7580

Table 1. Entangled Two-Dimensional Networks Containing Two-Membered Loops

	refcode	compd formula[a,b]	entanglement type[c]	layer topology:[d] sempl (2-c)	link type[e]	class[f]	year, ref
1	ANARIR	[Cd(**bcbpy**)(*bpdc*)$_{0.5}$Br]·7H$_2$O	INT-2f	**hcb** (2,4L1)	1.1	IIIa	2011, 40
2	ANAROX	[Cd(**bcbpy**)(*bpdc*)$_{0.5}$Cl]·7H$_2$O	INT-2f	**hcb** (2,4L1)	1.1	IIIa	2011, 40
3	BOBGEF	[Co$_2$(**1,3-bix**)$_2$(*bpea*)$_2$]	INT-2f	**hcb** (2,4L1)	1.1	IIIa	2008, 38
4	DAYMEX	[Mn$_4$(**pcp**)$_4$(*bpye*)(DMF)$_2$]	INT-2f	**sql** (2,6L1)[g]	1.2		2012, 41
5	DUCFOX	[Co$_2$(**btx**)$_2$(*btx*)(H$_2$O)$_4$(*β*-Mo$_8$O$_{26}$)]·2H$_2$O	INT-2f	**hcb** (2,4L1)	1.1	IIIa	2009, 42
6	DUCFUD	[Ni$_2$(**btx**)$_2$(*btx*)(H$_2$O)$_4$(*β*-Mo$_8$O$_{26}$)]·2H$_2$O	INT-2f	**hcb** (2,4L1)	1.1	IIIa	2009, 42
7	DUCHIT	[Zn$_2$(**btx**)$_2$(*btx*)(H$_2$O)$_4$(*β*-Mo$_8$O$_{26}$)]·2H$_2$O	INT-2f	**hcb** (2,4L1)	1.1	IIIa	2009, 42
8	ETEKUK	[Mn$_4$(**dbsf**)$_4$(*1,4-bix*)(H$_2$O)$_4$]·2H$_2$O	INT-2f	**sql** (2,6L1)[g]	1.2		2011, 43
9	ETELAR	[Ni(**dbsf**)(*bbi*)(H$_2$O)$_2$]·2H$_2$O	INT-2f	**hcb** (2,4L1)	1.1	IIIa	2011, 43
10	EVUSEU	[Zn(**Hapoxbda**)(*bpye*)]·(DMA)·(DMA)$_x$	INT-2f	**hcb** (2,4L1)	1.1	IIIa	2011, 44
11	EYEYIR	Zn(**Hcboxip**)(*bipy*)$_{1.5}$	INT-2f	**sql** (2,6L1)	1.1	IIIb	2011, 45
12	GALKIP	[Ni(**dbsf**)(*1,4-bix*)(H$_2$O)]·0.38H$_2$O	INT-2f	**hcb** (2,4L1)	1.1	IIIa	2012, 46
13	GUBZIN	[Mn$_2$(H$_2$O)$_4$(**btx**)$_2$(*btx*)(SiMo$_{12}$O$_{40}$)]·4H$_2$O	INT-2f	**hcb** (2,4L1)	1.1	IIIa	2009, 47
14	GUBZOT	[Ni$_2$(H$_2$O)$_4$(**btx**)$_2$(*btx*)(SiMo$_{12}$O$_{40}$)]·4H$_2$O	INT-2f	**hcb** (2,4L1)	1.1	IIIa	2009, 47
15	GUBZUZ	[Co$_2$(H$_2$O)$_4$(**btx**)$_2$(*btx*)(SiMo$_{12}$O$_{40}$)]·4H$_2$O	INT-2f	**hcb** (2,4L1)	1.1	IIIa	2009, 47
16	IQEJOE	[Cd(**cpmb**)(*bbi*)$_{0.5}$(H$_2$O)]	INT-2f	**sql** (2,6L1)	1.1	IIIb	2011, 48
17	KEZPIP	[Cd(**cpmb**)(*bbi*)$_{0.5}$(H$_2$O)]	INT-2f	**sql** (2,6L1)	1.1	IIIb	2007, 49
18	LALFOV	[Fe(**bipe**){*Au(CN)*}{ Au(CN)}·MeOH]	INT-2f	**hcb** (2,4L1)	1.1	IIIa	2010, 50
19	MARMID	[Co(**oba**)(*bib*)] ·H$_2$O	INT-2f	**sql** (2,6L1)	1.1	IIIb	2012, 51
20	MUNPIV	[Co(**bih**)(*bpdc*)]	INT-2f	**hcb** (2,4L1)	1.1	IIIa	2009, 52
21	MUNPUH	[Co(**1,4-bix**)(*bpdc*)]	INT-2f	**hcb** (2,4L1)	1.1	IIIa	2009, 52
22	NEBSUI	[Zn(**1,4-bix**)(*1,4-bix*)(NO$_3$)$_2$]·4.5H$_2$O	INT-2f	**hcb** (2,4L1)	1.1	IIIa	1997, 53
23	NUDDAS	[Zn(**1,2-bbomb**)(*bipy*)$_{0.5}$]	INT-2f	**sql** (2,6L1)	1.1	IIIb	2009, 54
24	OVIDAZ	[Zn(**cpds**)(*bipe*)$_{0.5}$	INT-2f	**sql** (2,6L1)	1.1	IIIb	2011, 55
25	QUQGOZ	[Zn$_3$(OH)$_2$(**dhbbdc**)$_2$(*bipy*)(H$_2$O)$_2$]·H$_2$O	INT-2f	**sql** (2,6L2)	1.1	IIIc	2010, 56
26	RUBGIF	[Ni(**dbsf**)$_2$(*bipy*)]·H$_2$O	INT-2f	**sql** (2,6L1)	1.1	IIIb	2009, 57
27	SULKEQ	[Zn(**dbsf**)$_2$(*bipy*)]·H$_2$O	INT-2f	**sql** (2,6L1)	1.1	IIIb	2009, 58
28	TAHNIB	[Zn$_2$(**dbsf**)$_2$(*bpimb*)]·H$_2$O	INT-2f	**sql** (2,6L1)	1.1	IIIb	2010, 59
29	TONFIM	[Cd$_2$(**1,4-bix**)$_2$(*dpb*)$_2$]	INT-2f	**hcb** (2,4L1)	1.1	IIIa	2008, 60
30	TONFOS	[Cd(**mbd**)(*bpimb*)$_{0.5}$(H$_2$O)]	INT-2f	**sql** (2,6L1)	1.1	IIIb	2008, 60
31	UYOHOG	[Mn$_4$(**dba**)$_4$(*1,4-bix*)]	INT-2f	**sql** (2,6L1)[g]	1.2		2011, 61
32	UZAWEY	[Cd$_4$(Hidc)$_2$Cl$_4$(**bbi**)$_2$(*bbi*)]	INT-2f	**sql** (2,6L1)	1.1	IIIb	2011, 62
33	WOCKOP	[Cd(**bpp**)(*tp*)(H$_2$O)]·*n*H$_2$O	INT-2f	**hcb** (2,4L1)	1.1	IIIa	2008, 63
34	WODGUS	[Cd$_2$(**pca**)$_2$(*bbi*)]	INT-2f	**sql** (2,6L1)	1.1	IIIb	2008, 64
35	YOCPEL	[Mn$_2$(**p-xbp**)$_2$(*p-xbp*)](ClO$_4$)$_2$	INT-2f	**sql** (2,6L1)	1.1	IIIb	1995, 65
36	NUDDEW	[Zn$_2$(**1,3-bbomb**)$_2$(*bipy*)]	INT-3f	**sql** (2,6L1)	2.2	IIId	2009, 54
37	TONGAF	[Zn(**obbd**)(*bpib*)$_{0.5}$]	INT-3f	**sql** (2,6L1)	2.2	IIId	2008, 60
38	WAGXAF	[Zn(**H$_2$tfpbbp**)(*fip*)]·H$_2$O	INT-3f	**hcb** (2,4L1)	2.1		2010, 66
39	WAGXEJ	[Zn$_2$(**H$_2$tfpbbp**)$_2$(*nip*)$_2$]·H$_2$O	INT-3f	**hcb** (2,4L1)	2.1		2010, 66
40	NUDDIA	[Zn$_4$(**1,2-bbomb**)$_4$(*bpp*)$_2$]	PPROT[h]	**sql** (2,6L1)	*i*	IVa	2009, 54
41	UHUROF	[Co$_2$(**pcp**)$_2$(*bpp*)]·2CH$_3$OH	PCAT[h]	**sql** (2,6L1)	*j*	IVb	2009, 67
42	BOBGIJ	[Cd$_4$(**1,4-bix**)$_4$(*bpea*)$_4$]·4H$_2$O	IPROT[k]	**hcb** (2,4L1)	1.1	IVc	2008, 38
43	CUXTIZ	[Zn(**Hcboxip**)(*bimb*)]·2H$_2$O	IPROT[l]	**hcb** (2,4L1)	1.1	IVc	2010, 68

[a]Ligands forming the 2-loops are shown in boldface type; ligands acting as rods are shown in italic type. [b]Abbreviations for ligands: bbi = 1,1′-butane-1,4-diylbis(1*H*-imidazole); bib = 1,4-bis(2- methylimidazol-1-yl)butane; bih = 1,1′-hexane-1,6-diylbis(1*H*-imidazole); bipe = 4,4′-ethane-1,2-diyldipyridine; bipy = 4,4′-bipyridine; bpib = 1,4-bis[2-(pyridin-2-yl)-1*H*-imidazol-1-yl]butane; bpimb = 2,2′-[1,4-phenylenebis(methylene-1*H*-imidazole-1,2-diyl)]dipyridine; bimb = 1,1′-(1,4-phenylene)bis(1*H*-imidazole); bpp = 4,4′-propane-1,3-diyldipyridine; bpye = 4,4′-ethene-1,2-diyldipyridine; btx = 1,1′-[1,4-phenylenedi(methylene)]bis(1*H*-1,2,4-triazole); p-xbp = 1,1′-[1,4-phenylenedi(methylene)]dipyridin-4(1*H*)-one; 1,4-bix = 1,1′-[1,4-phenylenedi(methylene)]bis(1*H*-imidazole); 1,2-H$_2$bbomb = 4,4′-[1,2-phenylenebis(methyleneoxy)]dibenzoic acid; 1,3-bix = 1,1′-[1,3-phenylenedi(methylene)]bis(1*H*-imidazole); 1,3-H$_2$bbomb = 4,4′-[1,3-phenylenebis(methyleneoxy)]dibenzoic acid; Hbcbpy = 1-(4-carboxybenzyl)-4-pyridin-4-ylpyridinium; H$_2$bpdc = biphenyl-4,4′-dicarboxylic acid; H$_2$dpb = 4-[(4-carboxybenzyl)oxy]benzoic acid; H$_2$fip = 5-fluoroisophthalic acid; H$_2$nip = 5-nitroisophthalic acid; H$_2$pca = 4,4′-methylenebis(3-hydroxy-2-naphthoic acid); H$_2$bpea = 4,4′-ethene-1,2-diyldibenzoic acid; H$_2$cpds = 6,6′-dithiodinicotinic acid; H$_2$cpmb = 3-[(4-methylbenzyl)amino]benzoic acid; H$_2$dba = 4,4′-methylenebis(benzoic acid); H$_2$dbsf = 4,4′-sulfonyldibenzoic acid; H$_2$dhbbdc = 4,4′-(1,2-dihydroxyethane-1,2-diyl)dibenzoic acid; H$_2$mbd = 4,4′-[methylenebis(oxy)]-dibenzoic acid; H$_2$oba = 4,4′-[1,2-ethanediylbis(oxy)]dibenzoic acid; H$_2$obbd = 4,4′-[oxybis(ethane-2,1-diyloxy)]dibenzoic acid; H$_2$pcp = 4,4′-[propane-1,3-diylbis(oxy)]dibenzoic acid; H$_2$tfpbbp = *N*,*N*′-[(2,3,5,6-tetrafluoro-1,4-phenylene)dimethylene]diisonicotinamide; H$_2$tp = terephthalic acid; H$_3$cboxip = 5-[(4-carboxybenzyl)oxy]isophthalic acid; H$_3$apoxbda = 5-[2-(acetylamino)-4-carboxyphenoxy]isophthalic acid; H$_3$idc = imidazole-4,5-dicarboxylic acid. [c]INT-2f = 2-fold interpenetrated; PPROT = parallel entangled polyrotaxane; IPROT = inclined entangled polirotaxane. [d]Notation: (2,6L1) corresponds to a 2,6-c net with point symbol $2^2.4^8.6^5$, (2,4L1) corresponds to a 2,4-c net with point symbol 2.6^5, and (2,4L2) corresponds to a 2,6-c net with point symbol $2^2.4^9.6^4$. [e]Rotaxane link type: 1.1 for one rod/one ring; 1.2 for one rod/two rings; 2.2 for two rods/two rings. [f]Classification according to Batten et al.[19] [g]Dimers. [h]Degree of catenation 2; index of separation 1. [i]Half loops 2.1 and half not threaded. [j]All 2-loops are catenated via Hopf links. [k]Degree of catenation 2/2; angle 31.9°. [l]Degree of catenation 2/2; angle 42.5°.

dx.doi.org/10.1021/cr500150m | *Chem. Rev.* 2014, 114, 7557−7580

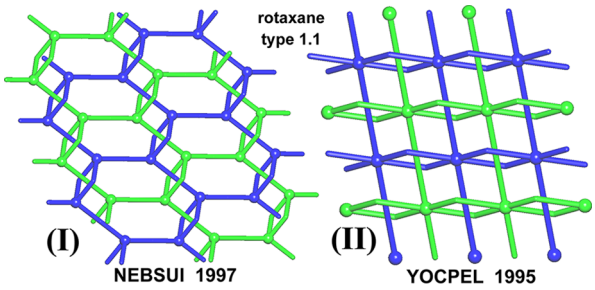

Figure 12. Two oldest examples of entanglement of polyrotaxane-like structures observed in the 1990s: NEBSUI[53] and YOCPEL.[65]

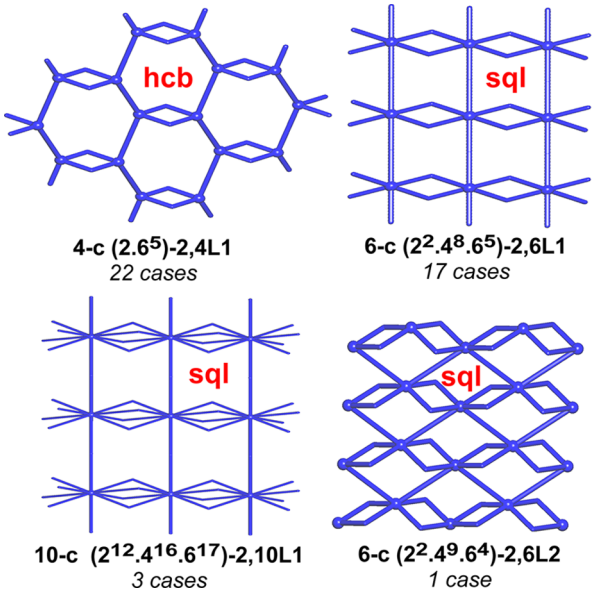

Figure 13. Four different layer topologies observed in polyrotaxane-like structures.

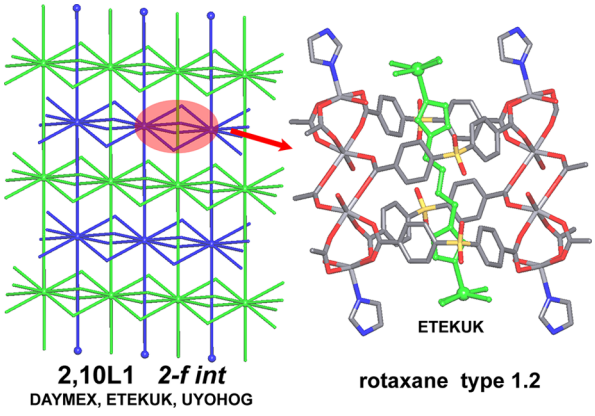

Figure 14. Unique rotaxane type 1.2 (one rod, two rings).

each rod threads two rings from different layers: we can call it type 2.2.

It must be stressed that these inextricable entanglements are completely distinct from the more usual topological classes discussed in the remainder of this review, though they are reminiscent of other entanglements of layers without 2-membered loops. All the species described can be classified as examples of "polythreaded interpenetration" (2D + 2D → 2D). On the other hand, a few other special cases have also been recently discovered containing 2D layers with 2-membered loops that, via the involvement of these rings, give 3D networks. As in the cases of polycatenation, they show an increase of dimensionality with respect to the basic constituent motifs (i.e., 2D + 2D → 3D) (see Figure 6). In two cases of these 2D + 2D → 3D entanglements (BOBGIJ[38] and CUXTIZ[68]), the layers interlace in an inclined fashion through rotaxane interactions of type 1.1. Two sets of parallel 2D layers of type 2,4L1 cross at an angle of 31.9° for BOBGIJ and 42.5° for CUXTIZ with polythreading to produce the 3D array. In both cases, all the 2-loops are threaded by rods of the inclined layers while only half of the single edges are involved in threading. We can describe these cases as "inclined entangled polyrotaxanes" (IPROT, see Table 1). Indeed, the two species show some differences if we consider the density of entanglement, since in BOBGIJ each window of a layer is interlaced with two layers of the inclined set (and vice versa), while in CUXTIZ each window of a layer is interlaced with three layers of the inclined set, as shown in Figure 16.

A quite different situation is observed in NUDDIA.[54] The topology of the 2D layers is of the 2,6L1 type but with two orientations of the loops (shown in red and yellow in Figure 17). The individual layers are entangled with two others (above and below) in a parallel fashion, giving an intriguing 2D + 2D → 3D architecture that resembles the cases of parallel polycatenation. Here, however, the links are two-rod rotaxanes (of type 2.1) that involve only half of the loops (the red ones in Figure 17) that are threaded by one rod of the upper and one rod of the lower layer. All the single edges of the layers are used in these threading interactions. This unique entanglement can be described as a "parallel entangled polyrotaxane" (PPROT, see Table 1), with an index of separation Is = 1 (see section 3.3 for the definition).

Also, UHUROF[67] is unique in that the 2-membered loops of its 2,6L1-type layers give Hopf links with the loops of two adjacent layers (above and below), thus resulting in a parallel polycatenated 3D array, with index of separation Is = 1 and degree of catenation Doc =2 (see section 3.3 for definition). This is made possible by the fact that the layers stack with mutual rotation, in an ABAB sequence (see Figure 18).[70]

3.3. Parallel Polycatenation

The results of the analysis using TOPOS show that there is a group of 127 cases that exhibit parallel polycatenation; that is, the 2D layers are interlaced in a parallel fashion by stacking with offset of their average planes. This type of entanglement is essentially made possible by the fact that the individual layers display a certain thickness. There are two reasons for the occurrence of thick sheets: they are markedly undulated versions of the planar 2D layers illustrated in Figure 3 or they are multiple layers (rigorously 2-periodic 3D), like those shown in Figure 4. The analysis of the distribution of topologies reveals that the thick layers (multiple layers) have a marked preference for the formation of entanglements with parallel polycatenation (85%; see Figure 7). The dominant topology in this type of entanglement is **sql** (54 out of the 127 examples), but the thick layers represent ca. 50% of all the cases (see Figure 7).

To achieve a better rationalization of these systems, we have introduced in a previous paper[2c] an index of the "degree of catenation" (Doc), defined by the number of motifs *n* entangled to each single motif; moreover, we have also suggested to establish within parallel polycatenation the number of motifs that must be "removed" in order to separate the whole array into two distinct parts (index of separation, Is). In almost all cases (with only five exceptions) we observe Doc = 2 and Is = 1; that is, each

dx.doi.org/10.1021/cr500150m | *Chem. Rev.* 2014, 114, 7557−7580

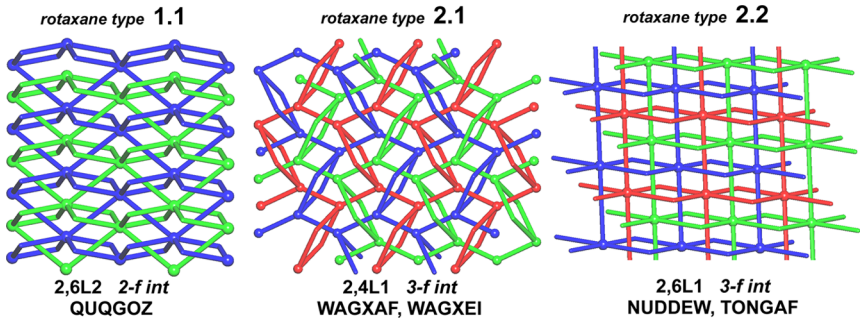

Figure 15. Three examples of interpenetrated polyrotaxane-like structures with different rotaxane type of entanglements of the 2-loops.

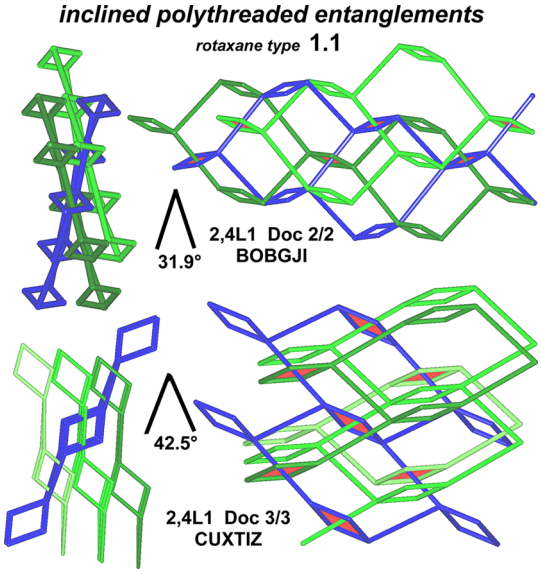

Figure 16. Two exceptional examples of inclined polythreaded entanglements.

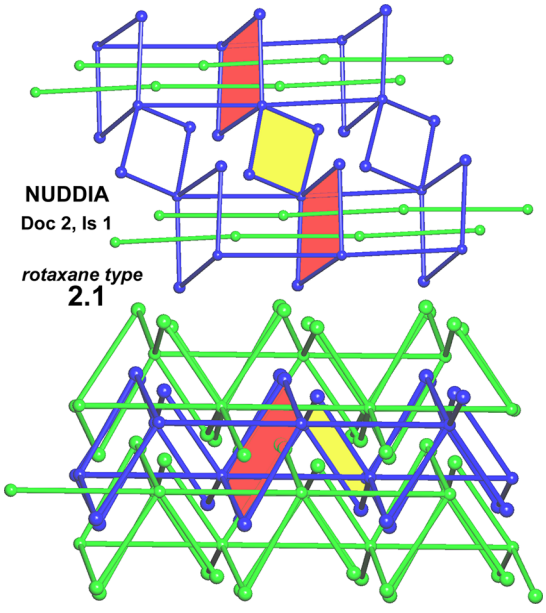

Figure 17. Unique example of parallel polythreaded entanglement.

layer is catenated with other two (the upper and lower nearest neighbors) and the array can be divided into two halves by elimination of one layer.

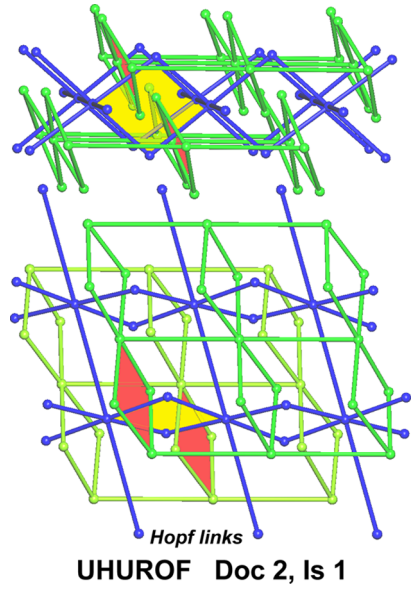

Figure 18. Unique example of parallel polycatenation via Hopf links of 2-loops.

It is worth mentioning briefly these five exceptional cases. In $[Cu(I)_2Cu(II)(bipy)_2(pydc)_2]\cdot 4H_2O$ [where bipy =4,4′-bipyridine and pydc = pyridine-2,4-dicarboxylate] (WUVBUK[71]), the individual motifs are **hcb** highly undulated layers (see Figure 19) that are catenated to four adjacent (two upper and two lower) layers, resulting in Doc = 4 and Is = 3.

On the other hand, $[Co_5(bipe)_9(H_2O)_8(SO_4)_4](SO_4)\cdot 14H_2O$ [where bipe =1,2-bis(4-pyridyl)ethane] (MEBBIE[72]) is com-

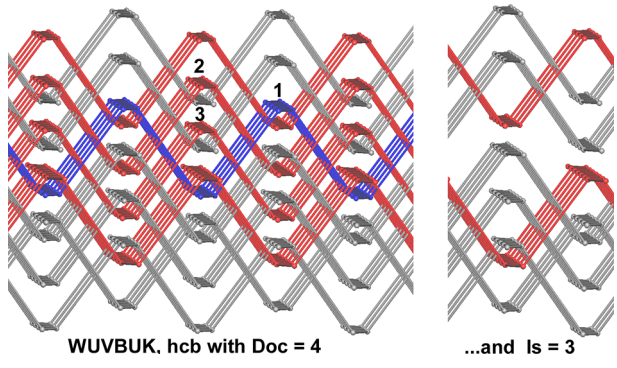

Figure 19. Exceptional case of parallel polycatenation observed in $[Cu^{I}_2Cu^{II}(bipy)_2(pydc)_2]\cdot 4H_2O$, showing Doc = 4 with the four red layers catenated with the reference one (blue) and the removal of three numbered layers resulting in Is = 3.

dx.doi.org/10.1021/cr500150m | Chem. Rev. 2014, 114, 7557−7580

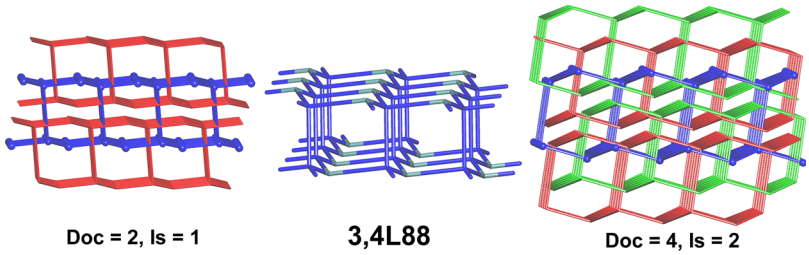

Figure 20. Thick layer 3,4L88 and its observed parallel polycatenation in seven structures.

posed of very high five-decked multiple 2D layers with a complex unique topology that can be described as a five-layer section of the chiral three-dimensional four-connected framework of (7^5.9)-**qzd** topology. These multiple layers are interlaced in parallel fashion with four such adjacent layers with indexes Doc = 4 and Is = 2 (see ref 72 for detailed figures).

Two other examples exhibit a high degree of catenation (Doc = 4, Is = 2):, Cu_4(dicyanamide)$_4$(bipy)$_3$(MeCN)$_2$ (LOTQUG[73]) and [Ag_3L_2][PF_6]$_3$·1.6THF·0.5C_6H_6·CH_2Cl_2 [where L= tetrakis(4-cyanophenyl)silane] (NORDAZ,[74]the first case of parallel polycatenation, reported in 1997). Both show the same 3,4L88 topology of their thick sheets that are bilayers representing a cut of diamond **dia** (see Figure 20). Bilayers with this topology are relatively common in this type of entanglement. There are five cases (XODJOQ,[75] BOQSEG,[76] BURGAX,[77] OKEJIY,[78] and WAVTEU[79]) all having Doc = 2 and Is = 1, very probably due to the decrease of cage dimensions. A special case is that of WUJDIO,[80] a puzzling species showing parallel polycatenation of KIa thick layers, with Doc = 2 but Is = 2, which will be discussed later.

A recent article[81] illustrates a rare breathing behavior supported by parallel polycatenation. Many dynamic porous systems have been characterized up to now evidencing that different mechanisms are at the origin of this phenomenon, also called gate-opening (with stepwise isotherms). Interestingly, these types of new adsorption profiles were first recognized for stacked 2D coordination layers.[82] In 2001, Li and Kaneko[82a] introduced the term "gate opening pressure" to explain the gas adsorption isotherms measured on the stacked square layers [Cu(bipy)$_2$(BF_4)$_2$] (bipy = 4,4′-bipyridine) that unusually showed no adsorption below the "gate pressure" value and a steep increase at this value.[83] In the same year Kepert and coworkers[84] reported an extensive gas and vapors adsorption study on the flexible interdigitated layers of (8^2.10)-KIa topology [Ni_2(4,4′-bipyridine)$_3$(NO_3)$_4$] showing step adsorption isotherms. After these early reports, many other examples of flexible 2D coordination networks have been reported.[85] It has been well documented that the dynamism in stacked 2D coordination networks is associated with expansion/shrinkage or sliding of the layers as well as the breathing phenomenon; it follows that 2D layers polycatenated (undulated or thick) may be good candidates for such dynamic behavior.[86]

3.4. Inclined Polycatenation

This is a quite large family of polycatenated 2D frames that include 222 cases, many of which were already reviewed in detail previously.[2a−c] It is the second largest group after that of interpenetrated arrays (29% vs 49%) as shown in Figure 7. The majority of these species consist of two identical sets of 2D parallel layers spanning two different stacking directions. They are characterized by an increase of dimensionality (2D → 3D) and each individual motif is catenated with an infinite number of other inclined layers but, obviously, not with all the frames contained in the 3D array.

Also for this type of entanglement we can define a "degree of catenation" (Doc), a symbol of type (*a*/*b*/...), where *a*, *b*, ... are the numbers of "external" rings catenated to a single ring in the first, second, ..., motif, in order of increasing value.[2c]

Analysis of the topologies of single 2D motifs shows that a limited number of nets is observed: **sql** (159), **hcb** (45), **fes** (10), 3,4L13 (4), 4,4L28 (1), and three with layers of different topologies (see below). The 3,4L13 and 4,4L28 topologies are illustrated in Figure 21. Cu_4(ODPA)$_2$(bpye)$_4$(H_2O)$_{10}$·2H_2O

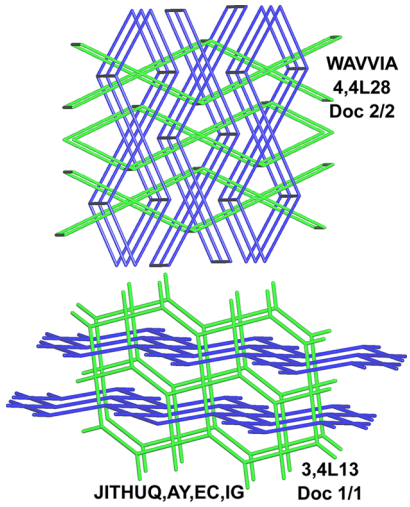

Figure 21. Rare topologies of inclined polycatenation observed in five structures.

[where H_4ODPA = 3,3′,4,4′-oxidiphthalic acid and bpye = 4,4′-ethene-1,2-diyldipyridine] (WAVVIA[87]) is a unique species exhibiting inclined polycatenation of thick layers (of 4,4L28 topology), at difference from what observed in parallel polycatenation where interlocking of thick layers is a common feature. 3,4L13 is a planar net observed for the four isomorphous M(MPDCO)(TPB)$_{0.5}$(H_2O)·(H_2O)$_x$, where MPDCO = 6-methylpyridine-2,4-dicarboxylic acid *N*-oxide, TPB = 1,2,3,4-tetra-(4-pyridyl)butane, and M = Co (JITHUQ), Ni (JITJAY), Zn (JITJEC), or Cd (JITJIG).[88]

Because the dominant topology of the layers is **sql** (more than 70%), particular attention has been devoted since the beginning to classification of the different ways of interlocking of two independent sets. Three possible arrangements have been suggested, with a largely accepted notation: parallel−parallel (p−p), parallel−diagonal (p−d), and diagonal−diagonal (d−d), depending on the relative orientation of the frames.[2c,89] A more detailed and automatic classification is possible with the new

dx.doi.org/10.1021/cr500150m | *Chem. Rev.* 2014, 114, 7557−7580

topological analysis of Hopf ring nets[21] that will be reported in future papers.

Within the inclined polycatenation category, many peculiar situations are observed that deserve greater attention. This is due to the possible presence of (I) layers of different nature (i.e., different by topology or by chemical composition or even only by ligand conformation that, moreover, can be present in different ratios), (II) more than two interlaced parallel stacking sets, or (III) unusual values of the Doc indexes. In some cases, a combination of more of the above features can be observed together.

Particularly intriguing are the three cases exhibiting inclined polycatenation of layers with different topologies that are illustrated in Figure 22. EHOVON,[90] $Ni_2(btec)(azpy)_2(H_2O)_6$]-

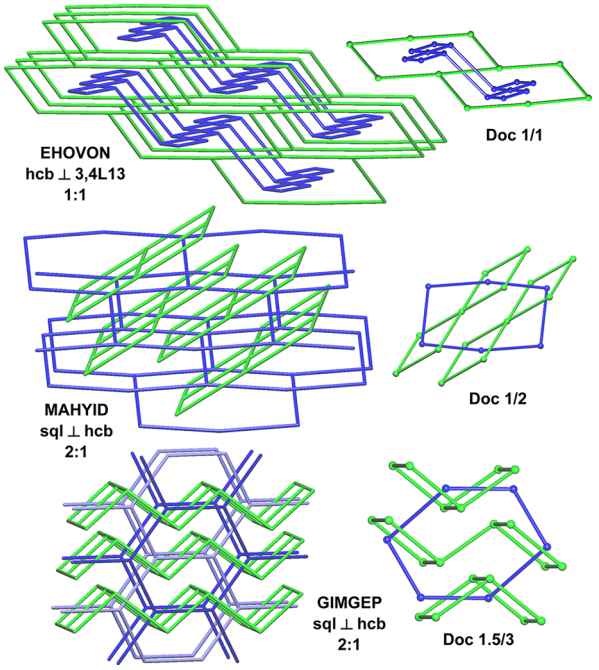

Figure 22. The only three cases exhibiting inclined polycatenation of layers with different topologies.

$[Ni_2(btec)(azpy)(H_2O)_4]$ [where H_4btec =1,2,4,5-benzenetetracarboxylic acid and azpy = 4,4′- azobis(pyridine)], contains **hcb** and 3,4L13 layers in ratio 1:1 and with Doc = 1/1. The other two cases, $[Ni(azpy)_2(NO_3)_2]_2[Ni_2(azpy)_3(NO_3)_4]$ (MAHYID[91]) and $[Zn(tp)(1,3\text{-bix})]_2[Zn_2(tp)_2(1,3\text{-bix})]$ (GIMGEP[92]) [where tp = terephthalate and 1,3-bix = 1,3-bis(imidazol-1-ylmethyl)benzene], both contain **sql** and **hcb** in ratio 2:1. This different ratio affects the values of Doc, which are 1/2 and 1.5/3, respectively. The latter noninteger value of Doc arises from the unique entanglement in GIMGEP: the **sql** are represented by two independent 4-rings that in total catenate with three 6-rings of **hcb** (3/2 = 1.5), while the unique 6-ring of the **hcb** catenates with three 4-rings of three **sql** (3), resulting in Doc 1.5/3.

Six species contain interlaced layers of the same **sql** topology but different chemical composition (MOVSEW,[93] SARFOH,[94] and VIRYIF[95]) or ligand conformation (MUPZON,[96] EWAXUV,[97] and KOLPEH[98]). In detail:

(1) VIRYIF:[95] Doc 1/1, ratio 1:1, $[Cu(bbi)_2][Cu(bbi)V_4O_{12}]$, where bbi =1,1′-(butane-1,4-diyl)bis(imidazole)

(2) MOVSEW:[93] Doc 1/2, ratio 1:1, rectangular and square **sql**, $[Cu_2(5\text{-HIPA})_2(4,4'\text{-bipy})_2(H_2O)_2][Cu_3(5\text{-HIPA})_2$(pyridine-2-carboxylate)$_2(bipy)_2(H_2O)_4]$, where 5-HIPA = 5-hydroxyisophthalate and bipy = 4,4′-bipyridine

(3) SARFOH:[94] Doc 0.5/1, ratio 1:2, rectangular and square **sql**, $[Co_2(pico)_2(4,4'\text{-bpy})(H_2O)_2][Co(pico)(4,4'\text{-bpy})]_2$, where pico = 3-hydroxypicolinate

(4) MUPZON:[96] Doc 1/2, ratio 1:2, $[Ni(bipe)(ip)(H_2O)]$-$[Ni(bipe')(ip')(H_2O)]_2$, where bipe = 1,2-bis(4-pyridyl)ethane and ip = isophthalate

(5) EWAXUV:[97] Doc 2/2, ratio 1:1, planar **sql** with different planar symmetry *c2mm* and *p4gm*, $[Cu(1,4\text{-bix})_2(SO_4)][Cu(1,4\text{-bix}')_2(SO_4)]$, where 1,4-bix = 1,4-bis(1-imidazolylmethyl)-benzene

(6) KOLPEH:[98] Doc 1/1, ratio 1:1, planar and undulated **sql**, $[Zn(dbsf)(bimb)][Zn(dbsf')(1,2\text{-bix}')]$, where H_2dbsf = 4,4′-dicarboxybiphenylsulfone and 1,2-bix =1,2-bis(1-imidazolylmethyl)benzene

Another peculiar situation consists of the presence of more than two (as usual) crossing sets of parallel layers, summarized in Figure 23. The analysis reveals that seven cases show this feature.

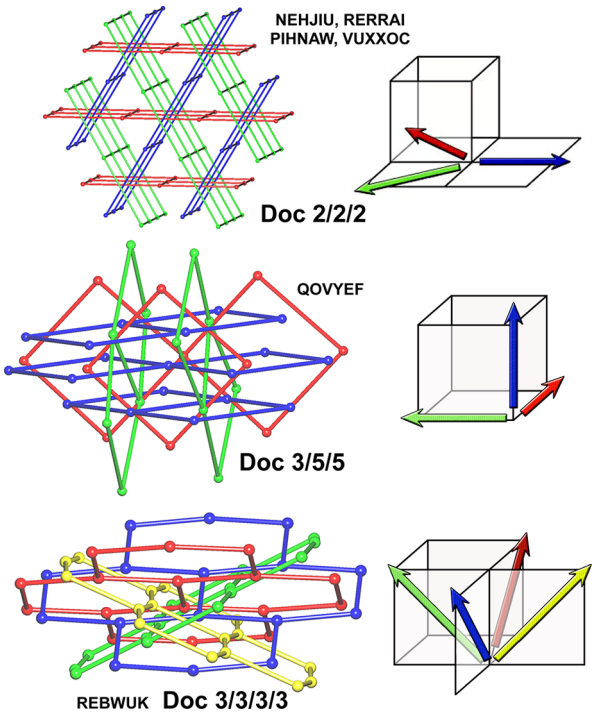

Figure 23. Inclined polycatenation with more than two crossing sets of parallel layers.

Five of them are composed of three sets of **sql** whose stacking directions lie coplanar; four of these have Doc 2/2/2 while Doc 2/2/4 is observed only for $\{[Ni(bipe)_2(H_2O)_2]_2[Ni_2(bipe)_3(H_2O)_6][Ni_2(bipe)_3(H_2O)_6]\}$-$(SO_4)_6$ [where bipe = 1,2-bis(4-pyridyl)ethane] (EJAXOC[99]), which presents the three **sql** in the ratio 2:1:1 with square:rectangular:rectangular windows. The simpler example of [Ni(4,4′-bipyridine)(4-carboxylatocinnamato)] (VUXXOC[100]) is illustrated in Figure 23). The other two cases (out of the seven) are different: $[Fe(bpb)_2(NCS)_2]$, where bpb = 1,4-bis(4-pyridyl)butadiyne (QOVYEF[101]), contains three sets of **sql** that stack in three perpendicular directions with ratio 1:1:2, giving a Doc of 3/5/5; and $[Co_2(4,4'\text{-azopyridine})_3(NO_3)_4]$ (REBWUQ[102]) exhibits four equal sets of **hcb**, whose stacking

dx.doi.org/10.1021/cr500150m | Chem. Rev. 2014, 114, 7557−7580

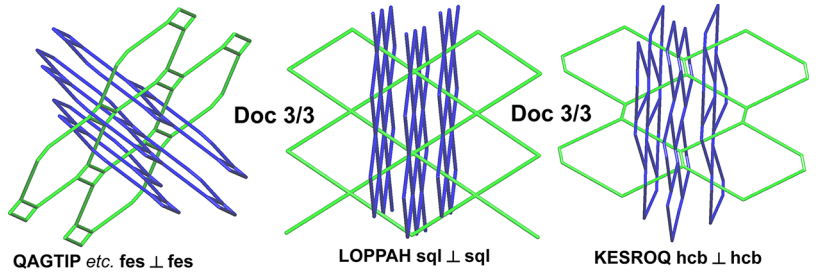

Figure 24. Topologies observed in 10 cases of inclined polycatenation with Doc = 3/3.

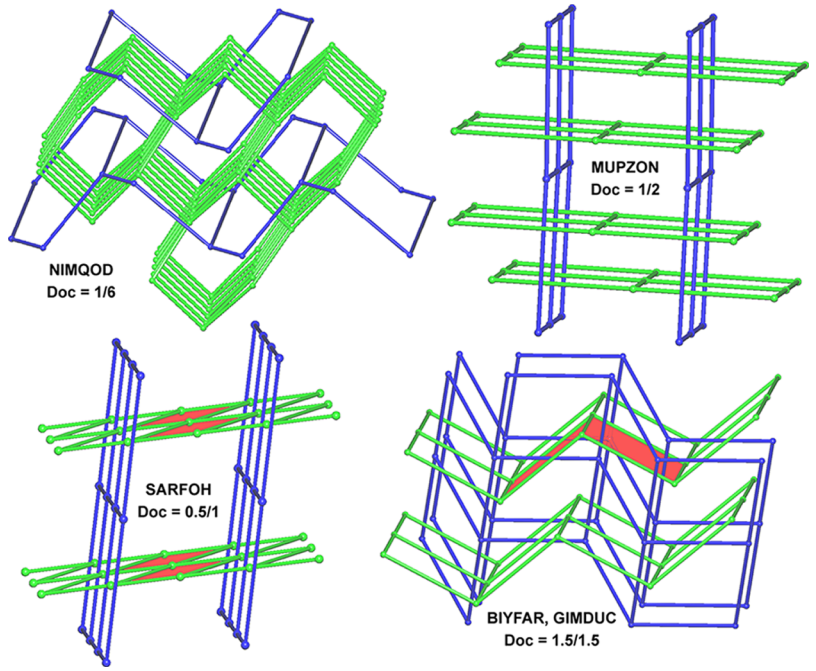

Figure 25. Inclined polycatenation examples with unusual values of degree of catenation. Highlighted in red are rings not catenated in SARFOH and the two rings with different catenation in BIYFAR and GIDMUC.

directions are disposed around a 4-fold crystallographic axis, giving a Doc of 3/3/3/3 (see Figure 23).

We can now briefly examine the values of the index Doc. The "normal" cases with Doc = 1/1 appear for 123 structures over 222, and markedly decrease upon passing to Doc = 2/2 (71 structures) and to Doc = 3/3 (12 structures). Within the "normal" cases the **sql** topology is dominant (86%), while in the cases with Doc = 2/2 the **sql** and **hcb** topologies are almost equally populated. With Doc = 3/3, the **fes** topology is observed 10 times versus one instance each for **hcb** and **sql**. All three distinct types are shown in Figure 24. The trend could be rationalized by considering that the increase in degree of catenation can be favored by an increase of the dimensions of the net windows upon passing from squares (**sql**) to hexagons (**hcb**) and finally to octagons (**fes**), on maintaining the same edge.

It is worth mentioning that there is only one case with Doc = 4/4: $[Zn_2(SO_4)_2(2,6\text{-ndc})(L)]$ [where 2,6-H_2ndc = 2,6-naphthalenedicarboxylic acid and L = *N*,*N*′-bis(pyridin-4-yl)hexanediamide] (OTUYAE[103]), based on **sql** layers with large rectangular meshes.

Particularly intriguing is the structure of $(CuCN)_{20}(piperazine)_7$ (NIMQOQ;[104] see Figure 25), with a strange Doc value of 1/6 that is based on the inclined polycatenation of two sets of **hcb** layers of quite different nature and dimensions. One layer contains very large rings consisting of $Cu_{18}(CN)_{16}(piperazine)_2$ macrocycles that are catenated by six layers of the second type, composed of hexagonal $Cu_6(CN)_4(piperazine)_2$ units.

Though generally all the windows of a layer show the same value of Doc, a few exceptions have also been observed and are illustrated in Figure 25. We have already mentioned GIMGEP,[92] with Doc = 1.5/3, among the three cases with layers of different topology (see Figure 23). Moreover, we can cite SARFOH,[94] where only half the square windows of one set are catenated and hence we can reasonably assume Doc = 0.5/1, and MUPZON,[96] where the different conformation of the ligand creates a different ratio of the **sql** with rectangular shape, giving an asymmetric catenation with Doc = 1/2. Similarly, in [M(terephthalato)-(bispyridylpropane)], where M = Co (BIYFAR)[105] or Zn (GIDMUC),[106] both with undulated **sql** topology, all layers have half the square windows doubly catenated and the remainder only singly catenated, hence Doc = 1.5/1.5.

The inclined polycatenation category shows many examples with interesting magnetic properties. Kepert and co-workers[107] studied a series of iron **sql** with Doc = 1/1 exhibiting inclination angles between layers in the range 53.5−90°. Two cobalt compounds with **sql** topology also show similar properties: SARFOH,[94] discussed previously, and UNEGEA,[108] with Doc = 2/2. Other interesting properties have been observed in this class, very probably due to the flexibility of the entanglement:

dx.doi.org/10.1021/cr500150m | *Chem. Rev.* 2014, 114, 7557−7580

breathing behavior,[109] solid state reaction [2 + 2] photodimerization between the inclined **sql** nets,[110] and single-crystal to single-crystal guest exchange in **hcb** with Doc = 2/2.[111]

3.5. Borromean Links

Molecular rings can give inextricable entanglements not only via topological Hopf links; an alternative way involving at least three closed circuits at a time is represented by the Borromean link (see Figure 26).The construction of molecular Borromean rings has

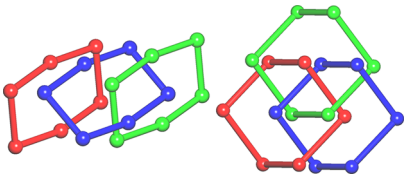

Figure 26. Two possible inextricable entanglements for a three-component link: on the left, the rings are entangled in couples by Hopf links (as observed in 6-rings from a 3-fold interpenetrated **hcb**); on the right, a Borromean link is presented.

been realized by Stoddart and co-workers[112] with an all-in-one synthetic strategy. The existence of Borromean links (instead of the usual Hopf links) in entangled coordination frameworks was noticed some years ago.[2c,20] This finding has probably stimulated investigations on the subject, and since then several new examples have been discovered in the area of coordination polymers (see Table 2).

Many studies have also been devoted in recent years to the rational synthesis of Borromean networks of organic molecular species via weak contacts, including a variety of supramolecular interactions like hydrogen bonds, halogen bonding, $\pi\cdots\pi$ stacking, and M···M (metallophilic) interactions. To build Borromean structures, the honeycomb net (**hcb**) seems essential in any synthetic strategy.[113]

In Table 2 we report only the species sustained by coordinative bonds and belonging to the realm of coordination frameworks. These include 2D (15 cases) and 3D (12 cases) Borromean entanglements. Four other examples exhibiting peculiar features are also listed; moreover, two cases have also been recognized, for the first time, to contain 5-Borromean coplanar entanglements with a complex "non-Brunnian" link (see below).[135]

All the individual layers show the **hcb** topology, and as is well-known,[20] in these arrays (except in MUHVOB and MUHVOB01)[125] each layer is entangled with two others (one "above" and one "below"). Adjacent layers, however, are not catenated but are linked via Borromean links, in which no two individual rings are interlocked.

These links can produce 2D Borromean entanglements (2D → 2D) (Figure 27) as well as 3D entanglements (2D → 3D) (Figure 28). In the 2D entanglements a finite number of layers ($n \geq 3$) are interlocked by means of n-Borromean links, while in the 3D entanglements the whole array represents an infinite case of n-Borromean links (Figure 28). Chains of rings of this kind are such that no one ring is catenated to other ones (Doc = 0) but cannot be separated. In both cases we have two possibilities: (i) the array can be completely separated into the component motifs by eliminating only one layer, that is, it possesses the "Brunnian" property (we define this as a n-Brunnian system);[136] or (ii) the array does not show the Brunnian property, that is, the elimination of one motif does not separate the system into free components (as in a n-Borromean system like the chain in Figure 28, where one elimination splits the system into two halves but leaves all the other motifs inextricably entangled). Obviously three Borromean rings, as well as any 3-fold 2D Borromean array, must have the Brunnian property (Figure 27).

The major group (15 entries) in Table 2 consists of 2D 3-fold entangled Borromean layers. They are usually characterized by the presence of moderately undulated honeycomb layers (of a certain thickness, range from 3.0 up to ca. 9.6 Å); this structural feature is very probably the main factor that favors the formation of 2D versus 3D systems, which always exhibit highly undulated layers (range from 9.4 up to ca. 19.8 Å) (see below).

It is worth mentioning here the case of DOJFUD, $(CuCl)_2(\eta^2,\eta^2$-p-divinylbenzene), reported many years ago in 1985.[137] Our analyses have revealed that if we consider as nodes the Cu_3Cl_3 hexagonal units [Cu−Cl edges of 2.275(3) and 2.323(3) Å] and as spacers the (Cu-η^2 bonded) p-divinylbenzene molecules, we obtain **hcb** layers that give a 2D Borromean entanglement. To the best of our knowledge, this is the oldest example of such entanglement that we were able to find within coordination networks. However, any Cu_3Cl_3 hexagon is superimposed on an identical (but rotated) unit, thus giving a hexagonal prismatic Cu_6Cl_6 cluster with interhexagonal distances [Cu−Cl 2.757(3) Å] much longer than the analogous intra-hexagonal contacts. When these interactions (ca. 0.4 Å shorter than the sum of van der Waals radii) are also taken into account, the whole array becomes a unique 2D self-catenated complex sheet. Due to this uncertainty (or arbitrary selection), we have decided to exclude DOJFUD from Table 2.

The honeycomb nets of these 2D layers are rather distorted with respect to the ideal planar geometry, and instead a chair conformation of the 6-ring is observed (see Figures 27 and 28).

In principle, 2D layers of any topology could be linked into Borromean entanglements, and some theoretical examples involving motifs with **sql** windows (like ladders) were previously suggested.[20] Though all the reported cases (within coordination polymers) contain layers with the same **hcb** topology, a noteworthy species has been recently described: [Ni(H$_2$O)$_4$(Bpybc)(phthalate)]·9H$_2$O [where Bpybc = 1,10-bis(4-carboxybenzyl)-4,4′-bipyridinium] (UGUGAF[138]), which is sustained by H-bonds joining dimeric Ni_2 nodes and reveals the Borromean interlacing of three **sql** layers (see Figure 29).

In the 3D Borromean entanglements (12 entries), the adjacent highly undulated layers are displaced along the stacking direction, a difference from the 3-fold 2D Borromean arrays where all the layers share the same average plane. The layers are characterized by hexagonal windows in the chair conformation with very long edges; it comes out that they display a pronounced thickness (see Table 2) that can favor the interlacing of adjacent layers.

As in the case of the 2D species YUXGOO,[126] Borromean entanglements seem favored by the presence of argentophilic Ag···Ag short contacts (well below the sum of the van der Waals radii of two Ag atoms), as evidenced in the 3D HOFXOP and HOFXUV.[128] In these species the silver nodes show interlayer Ag···Ag unsupported interactions of 2.934(2) and 2.946(2) Å, respectively. When these argentophilic contacts within the bonding scheme are also taken into account, indeed, a single 3D array results (as suggested by the authors): the unique self-catenated **dia**, a nonambient isotopic embedding of the diamondoid net.[2e,h,20]

The structure of 3D WIYMIA[131] is exceptional in that the edges of the **hcb** layers are "rotaxane-like" units with threaded cucurbituril molecular beads. It is therefore a unique example of

dx.doi.org/10.1021/cr500150m | Chem. Rev. 2014, 114, 7557−7580

Table 2. Borromean Linked Arrays

	refcode	compd formula[a]	entanglement	recognized by authors (Y/N)	layer topology, stacking direction, node	edge of **hcb** (Å); thickness[b] (Å)	space group	year, ref
1	DAPPAN	$\{[Ni(hatcd)]_3(tcba)_2\}$	BOR (2D → 2D)	Y	**hcb**, [001], $tcba^{3-}$	18.12; 7.05	$R\bar{3}$	2012, 114
2	GUWXIF	$\{Ni(cyclam)]_3(tcpeb)_2\}\cdot 6py\cdot 4H_2O$	BOR (2D → 2D)	N	**hcb**, [102], $tcpeb^{3-}$	24.90 and 25.08; 3.43	$P2_1/c$	2003, 115
3	ICIWOG	$[Cu(tmeda)]_2[Au(CN)_2]_3ClO_4$	BOR (2D → 2D)	N	**hcb**, [001], Cu	10.12 and 10.20; 6.78	$R32$	2001, 116
4	IWENII	$[Zn(bmb)(tp)_2\cdot 3H_2O$	BOR (2D → 2D)	Y	**hcb**, [010], Zn	11.12, 14.69, and 11.00; 5.78	$P\bar{1}$	2011, 117
5	LIKBIR	$[WOS_3Cu_3(bipy)_3]I$	BOR (2D → 2D)	Y	**hcb**, [001], WOS_3Cu_3 cluster	15.27; 8.80	$R\bar{3}c$	2007, 118
6	NEQDET	$[Ag_2(bismin)_3](CF_3SO_3)_2$	BOR (2D → 2D)	Y	**hcb**, [001], Ag	14.62, 3.22	$P\bar{3}$	2006, 119
7	PUNRUM	$[Zn_2(bppu)_3](SO_4)_2\cdot xH_2O$	BOR (2D → 2D)	Y	**hcb**, [001], Zn	17.81, 9.47	$R\bar{3}$	2010, 120
8	RESHUT	$[Hg^1I_2(bippyr)Hg^2I_2(bippyr)_{0.5}]$	BOR (2D → 2D)	Y	**hcb**, [011], Hg^1	15.55, 22.42, and 20.18; 8.92	$P\bar{1}$	2006, 121
9	SAVCAU	$[Ag_2(bismin)_3](BF_4)_2$	BOR (2D → 2D)	Y	**hcb**, [001], Ag	14.30; 3.06	$P\bar{3}$	2005, 122
10	TANJEZ	$[(Cu_4I_4)_2(biethiop)_3(H_2O)_2]\cdot 4H_2O$	BOR (2D → 2D)	N	**hcb**, [001], Cu_4I_4 cluster	19.31; 9.58	$R\bar{3}c$	2011, 123
11	WOCXIW	$[Ag_2(ethapu)_3](NO_3)_2\cdot 2MeCN\cdot xS$	BOR (2D → 2D)	Y	**hcb**, [001], Ag	16.39 and 16.04; 3.40	$C2/c$	2008, 124
12	WOCXOC	$Ag_2(ethapu)_3](NO_3)_2\cdot 7H_2O$	BOR (2D → 2D)	Y	**hcb**, [001], Ag	16.39 and 16.04; 3.81	$P2_1/c$	2008, 124
13, 14	MUHVOB/01	$[Pb_2(obed)_2(bipy)]$	BOR–5f (2D → 2D)	N	**hcb**, [100], Pb	12.31 and 17.95; 5.14	$P2_1/c$	2009, 125
15	YUXGOO	$[Ag_2(bisox)_3](ClO_4)_2$	BOR (2D → 2D)	Y	**hcb**, [001], Ag	15.14; 3.00[c]	$P\bar{3}$	2010, 126
16	AHIDEA	$[Ag_2(bipycox)_3OH][ClO_4]\cdot 2.5H_2O$	3D BOR (2D → 3D)	N	**hcb**, [001], Ag	18.54, 18.72, and 19.08; 16.61	$P32$	2002, 127
17	HOFXOP	$[Ag_2(H_2bisalic)_3](NO_3)_2$	3D BOR (2D → 3D)	N	**hcb**, [001], Ag	12.88; 9.41[d]	$R\bar{3}$	1999, 128
18	HOFXUV	$[Ag_2(H_2bisalic)_3](ClO_4)_2$	3D BOR (2D → 3D)	N	**hcb**, [001], Ag	12.13; 9.49[d]	$R\bar{3}$	1999, 128
19	KAVDAN	$[(bpybc)_3Mn_2(H_2O)_6](OH)_4\cdot 15H_2O$	3D BOR (2D → 3D)	N	**hcb**, [001], Mn	22.19; 19.74	$R\bar{3}$	2005, 129
20	KAVDER	$[(bpybc)_3Ni_2(H_2O)_6](OH)_4\cdot 15H_2O$	3D BOR (2D → 3D)	N	**hcb**, [001], Ni	21.86; 19.37	$R\bar{3}$	2005, 129
21	KAVDIV	$[(bpybc)_3Co_2(H_2O)_6](OH)_4\cdot 15H_2O$	3D BOR (2D → 3D)	N	**hcb**, [001], Co	22.00; 19.48	$R\bar{3}$	2005, 129
22	UZAZUR	$[Zn_4(bpybc)_6(H_2O)_{12}](OH)_8\cdot 9H_2O$	3D BOR (2D → 3D)	N	**hcb**, [001], Zn	22.03; 19.67	$R\bar{3}$	2011, 130
24	YANWOB	$[Eu_4(bpybc)_6(H_2O)_9(SO_4)_3]\cdot(OH)_6\cdot 51.5H_2O$	3D BOR (2D → 3D)	Y	**hcb**, [001], Eu	22.22; 19.54	$R\bar{3}$	2012, 132
25	YANWUH	$[Mn_4(bpybc)_6(H_2O)_{12}](tp)_3\cdot(OH)_2\cdot 30H_2O$	3D BOR (2D → 3D)	Y	**hcb**, [001], Mn	22.10; 19.82	$R\bar{3}$	2012, 132
26, 27	YANXAO/01	$[Mn_2(bpybc)_3(H_2O)_6](SO_4)_2\cdot 21H_2O$	3D BOR (2D → 3D)	Y	**hcb**, [001], Mn	22.32; 18.44	$R\bar{3}$	2012, 132
28	GIQGAP	$\{[Ag_3(tibimt)_2][Ag_2(tibimt)_2)]\}(SbF_6)_5\cdot CHCl_3\cdot H_2O$	2D + 2D BOR + 2D	Y	For 2D BOR: **hcb**, [001], tibimt. For 2D: **hcb**, [001], tibimt and Ag.	For 2D BOR: 19.89; 8.88. For 2D: 10.67; 2.88.	$P6_322$	2007, 133
29	GIQGET	$\{[Ag_3(tibimb)_2][Ag_2(tibimb)_2)]\}(SbF_6)_5\cdot 1.5H_2O$	2D + 2D BOR + 2D	Y	For 2D BOR: **hcb**, [001], tibimb. For 2D: **hcb**, [001], tibimb and Ag.	For 2D BOR: 19.95; 8.76. For 2D: 10.81; 3.13.	$P6_322$	2007, 133
30	ISAROK	$[Ag_2(bisox)_3](BF_4)_2\cdot 1.2Et_2O$	2D BOR/cage	Y	**hcb**, [001], Ag	14.72; 3.06[e]	$P6_3/m$	2011, 134
31	YUXGUU	$[Ag_2(bisox)_3](ClO_4)_2\cdot 1.2Et_2O$	2D BOR/cage	Y	**hcb**, [001], Ag	14.76; 3.04[f]	$P6_3/m$	2010, 126

[a]Abbreviations for ligands: biethiop = 4,4′-bis(ethylthiomethyl)biphenyl; bippyr = *N*,*N*′-bis(4-pyridylmethyl)pyromellitic diimide; bipy = 4,4′-bipyridine; cox = *N*,*N*′-Bis(3-pyridinecarboxamide)-1,6-hexane; bismin = 1,4-bis[(2-methylimidazol-1-yl)methyl]benzene; bisox = 1,4-bis[(3,5-dimethylisoxazol-4-yl)methyl]benzene; bmb = 1,4-bis(2-methylbenzimidazol-1-ylmethyl)benzene; bppu = *N*,*N*′-bis(3-pyridyl)-p-phenylenebis(urea); CB = cucurbit[6]uril; cyclam = 1,4,8,11-tetraazacyclotetradecane; ethapu = L1 = *N*,*N*″-ethane-1,2-diylbis(3-pyridin-3-ylurea); hactd = 3,10-bis(2-fluorobenzyl)-1,3,5,8,10,12-hexaazacyclotetradecane; tibimb = 1,3,5-tris{4-[(2-methylbenzimidazol-1-yl)methyl]phenyl}benzene; tibimt = 2,4,6-tris{4-[(2-methylbenzimidazol-1-yl)methyl]phenyl}-1,3,5-triazine; tmeda = *N*,*N*,*N*′,*N*′-tetramethylethylenediamine; H_2bisalic =*N*,*N*′-bis(salicylidene)-1,4-diaminobutane; H_2bpyab$(NO_3)_2$ = *N*,*N*′-bis(4-carboxyphenyl)-1,4-diammoniobutane dinitrate; H_2bpybcCl_2 = 1,1′-bis(4-carboxybenzyl)-4,4′-bipyridinium dichloride; H_2obed =3,3′-[oxybis(ethane-2,1-diyloxy)]dibenzoic acid; H_2tp = terephthalic acid (1,2-benzenedicarboxylic acid); H_3tcba = tri(4-carboxybenzyl)amine; H_3tcpeb = 1,3,5-tris[2-(4-carboxyphenyl)-1-ethynyl]benzene; Et_2O = diethyl ether; py = pyridine. [b]Thickness is evaluated as the distance between the two planes passing through the nodes of the **hcb** layer. [c]Ag···Ag = 2.999 Å. [d]With Ag···Ag interactions self-catenated **dia**. [e]Ag···Ag = 3.06 and 3.32 Å. [f]Ag···Ag = 3.04 and 3.32 Å.

dx.doi.org/10.1021/cr500150m | Chem. Rev. 2014, 114, 7557–7580

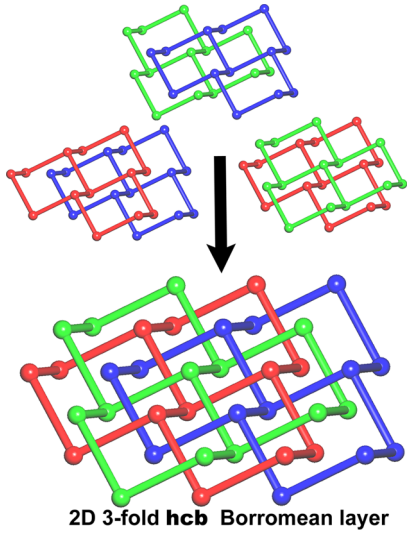

Figure 27. 2D Borromean entanglement showing the Brunnian property.

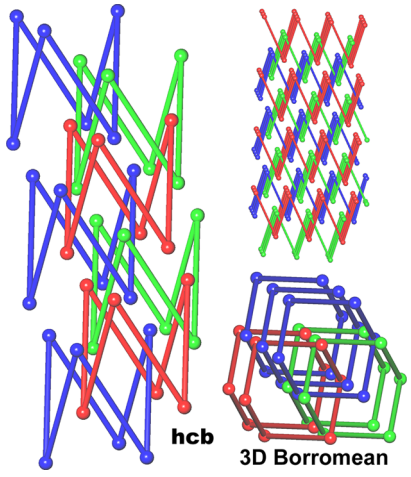

Figure 28. 3D Borromean entanglement observed (notice that it is not Brunnian).

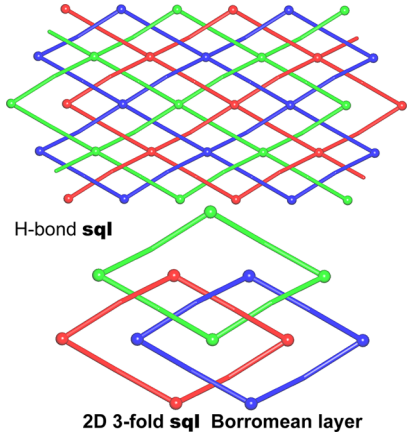

Figure 29. 2D Borromean entanglement of **sql** observed in H-bonded UGUGAF.

"Borromean polyrotaxane", unnoticed by the authors (Figure 30).

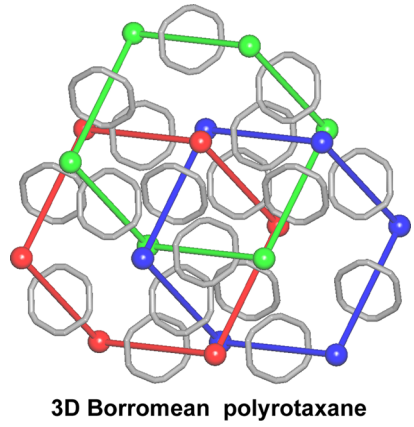

Figure 30. Exceptional 3D Borromean polyrotaxane: gray rings represent cucurbituril molecules.

Four species containing 2D Borromean 3-fold entangled layers should be discussed separately because they exhibit particular and fascinating additional structural features. In the pair GIQGAP and GIQGET,[133] there are two distinct types of **hcb** networks in the same crystal: one is a single **hcb** net with shorter edges and rather flat conformation, while the second one has longer edges and a chair conformation and is involved in a 3-fold Borromean entanglement. The crystal packing consists of stacking of the Borromean layers intercalated by two single layers that are placed face-to-face on the two sides of the Borromean entanglements, thus giving "sandwiched Borromean sheets" (Figure 31). These two species could be also included in the table of mixed entanglements discussed in section 3.6. Another pair of (very similar) compounds, ISAROK[134] and YUXGUU,[126] show interesting structures consisting of 2D Borromean layers intercalated by Ag_2L_3 cages (with the same composition of the **hcb** layers) that join adjacent entangled sheets via weak argentophilic contacts. Pillaring of 2D Borromean sheets is also observed in $[Cd_3(bfcs)_3(tttmb)_2(H_2O)_4]\cdot 8H_2O$ [where tttmb = 1,3,5-tris(1,2,4-triazol-1-ylmethyl)-2,4,6-trimethylbenzene and H_2bfcs = 1,1′-bis(3-carboxy-1-oxopropyl)-ferrocene] (FUWVUP)[139] with interlayer ferrocenyl bridges. The same type of bridge is present also within the Borromean sheets (intralayer), leading to an array defined by the authors as "interlocked Borromean layers", which overall results in a single trinodal self-catenated 3D net of topology 3,4,4T93. For this reason we have not included FUWVUP in Table 2.

In very recent times, several entanglements based on *n*-Borromean links have been observed that exhibit increased complexity. There is an entire world to be discovered in the future of new intriguing and stimulating entangled systems of this type that will need some rationalization.[140] For example, the exciting case of MUHVOB (and of the identical MUHVOB01)[125] represents an important topological novelty, in that it is, at present, the unique example of a 2D 5-Borromean entanglement. It consists of the interweaving of five coplanar **hcb** layers joined exclusively via Borromean links (the authors described the system simply in terms of 2D 5-fold interpenetration). Similar to the more usual 3-Borromean (3-Brunnian) sheets, all the layers share the same average plane, but in contrast, the entanglement is drastically more complex and non-Brunnian.

In the analysis of these complex links, a somewhat helpful approach may be the complete characterization of topological properties of the "basic" or "fundamental" link that comprises all

dx.doi.org/10.1021/cr500150m | *Chem. Rev.* 2014, 114, 7557−7580

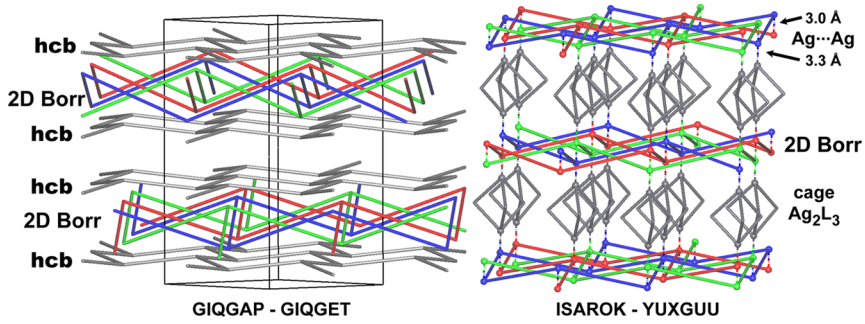

Figure 31. Alternated 2D Borromean layers.

the rings entangled with the basic one (if there is only one independent ring), illustrated in Figure 32. Using the concepts of

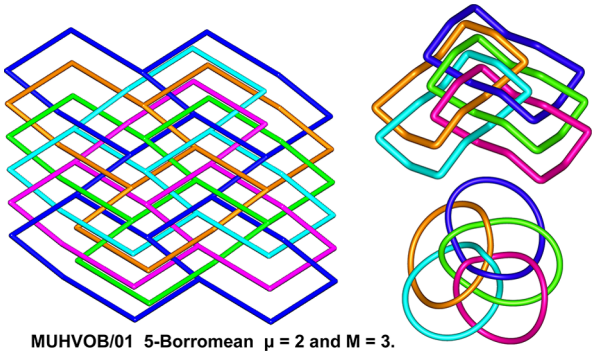

Figure 32. 2D 5-Borromean non-Brunnian layers.

the knots and links theory, we can follow the suggestions by Liang and Mislow[135] in order to find a cutting pathway and the relevant Brunn's cutting numbers μ and M. The minimum cutting number μ is the smallest number of cuts that suffice to unlink all the remaining uncut links, while the maximum cutting number M is the largest possible number of cuts that can be applied to unlink all the remaining uncut rings. Thus, the distinction between Borromean links with and without the Brunnian property is that $\mu = M = 1$ for the former and $M > 1$ for the latter.

In the present case (see Figure 32), elimination of one ring leaves five possible different, all nontrivial 4-Borromean links, while elimination of two rings produces 10 different entanglements of which five are trivial and five are 3-Borromean links. Thus, $\mu = 2$ and $M = 3$. These results are referred to the single 5-Borromean fundamental link. Obviously, it comes out that if the fundamental link is non-Brunnian, the same holds for the entire entanglement. Other extrapolations from the fundamental link to the whole entanglement, on the other hand, are difficult to formulate, and further studies on this subject are surely needed. It seems also that if we remove two selected appropriate layers we can get three separated layers, so by analogy Is = 2.

An even more complex case is that of the H-bonded organic molecules in the cocrystal [2TCA·3dpyb] [where TCA = 1,3,5-tris(4-carboxyphenyl)adamantane and dpyb = 1,4-di(pyridin-4-yl)benzene] (FUYBUX[141]) that we must mention here because of its intriguing topology, though it does not belong to the realm of coordination networks observed in this review. Again the structure is composed of parallel honeycomb layers that are entangled exclusively via Borromean links to give an overall 3D system (2D→ 3D). We can rationalize the array as consisting of stacked 7-fold entangled sheets (see Figure 33).

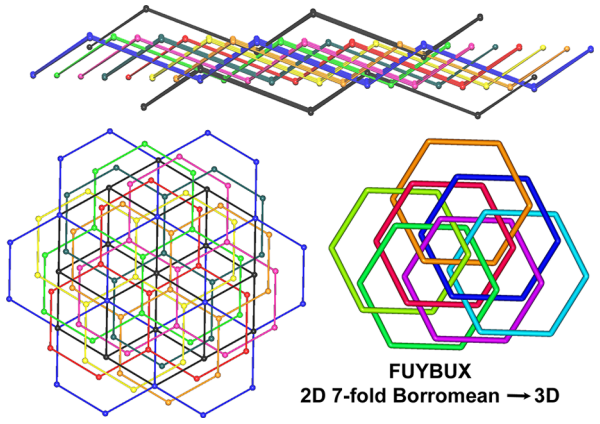

Figure 33. 3D Borromean entanglement of 2D 7-fold Borromean in the H-bonded FUYBUX. At the top, a side view of a 7-fold Borromean sheet is illustrated that reveals also the interlink of one motif of the central 7-fold sheet with one motif of the adjacent upper and one motif of the lower identical sheets.

These 7-Borromean sheets contain seven **hcb** coplanar layers. Thus, we can interestingly compare the fundamental link in three situations of increasing complexity that contain three (any 3-Borromean), five (MUHVOB), and seven (FUYBUX) layers that share the same average plane but show a growing number of triplets involved in the entanglement (1, 10, and 35 per fundamental link, respectively). A triplet is a system comprising three Borromean linked rings; the number of triplets can be assumed as the number of combinations (via Borromean links) of N rings taken three at a time.

Moreover, these 7-Borromean sheets are interlinked with the two adjacent (upper and lower) sheets via other Borromean links. In detail, each individual layer of a 7-fold sheet is linked with two individual motifs of the upper and with two of the lower entangled sheet, resulting in this way in an overall 3D architecture. The situation can be compared with that of the previously described 3D Borromean species (in Table 2), with the notable difference [2D (7-fold) → 3D] instead of [2D (single) → 3D].

3.6. Mixed Types of Entanglement of 2D Motifs

In this last section, we examine the possible presence of more than one type of entanglement of 2D motifs (equal or different in nature) in the same crystal species. In the previous sections we have underlined that the entanglements can involve 2D layers that differ in topology, composition, or conformation of the ligands but that are entangled in one manner only. A very limited number of cases, however, cannot be included in the above listed groups (illustrated in Figure 7) because of the contemporary

dx.doi.org/10.1021/cr500150m | Chem. Rev. 2014, 114, 7557−7580

Table 3. Mixed Entanglements of 2D Layers

	refcode	compd formula[a]	type of entanglement[b]	layer topology, stacking direction, node	year, ref
1	ACUCAC	$[Zn_4(peba)_8]\cdot(Hpeba)\cdot H_2O$	INT-2f (A) /2D (B)/2D (C)[c]	**sql**, [001], Zn	2001, 142
2	FAGCAS	$[Ag(bpp)_2]AsF_6$	INT-2f (A)/2D (B)[d]	**sql**, [001], Ag	2002, 143
3	FAGCEW	$[Ag(bpp)_2]PF_6$	INT-2f (A)/2D (B)[d]	**sql**, [001], Ag	2002, 143
4	VAMXEO01	$[Zn_3(tp)_3(bphy)_3]\cdot 2DMF\cdot 10H_2O$	INT-2f (A)/2D (B)[d]	**sql**, [010], Zn	2012, 144
5	ISABUZ	$[Ag(tcphb)(CF_3SO_3)]\cdot 0.5H_2O$	PCAT of INT-2f[e]	**hcb**, [010], Ag and tcphb	2004, 145
6	VAJSIK	$[Zn(nip)(1,4\text{-bpeb})]\cdot 2H_2O$	PCAT of INT-2f[e]	**sql**, [10−1], Zn	2010, 146
7	WAPCIB	$Cd_2(nbpdc)_2(1,3\text{-bix})_2H_2O$	PCAT of INT-2f[e]	3,4L127, [001], Cd	2012, 147
8	KAXTUA	$[Ag_6(tipa)_4(\beta\text{-}Mo_8O_{26})][H_2(\beta\text{-}Mo_8O_{26})]\cdot 5H_2O$	PCAT of INT-2f[f]	3,3L20, [112], Ag and tipa	2012, 148
9	MATJIC	$[Ni_5(pda)_5(bpp)_5]\cdot 12H_2O$	PCAT of INT-2f[f]	**sql**, [001], Ni	2012, 149
10	OHAYOM	$[Zn(mfda)(bpp)]$	PCAT of INT-2f[f]	**sql**, [010], Zn	2009, 150
11	XOPLEU	$[Cd(pyada)_2(ClO_4)_2(CH_3CH_2OH)_2]$	PCAT of INT-3f[g]	**sql**, [001], Cd	2009, 151
12	VUHCUX	$[Ag_3(tppt)_2](ClO_4)_3\cdot 8DMSO$	PCAT of INT-3f[h]	**hcb**, [102], tppt	2009, 152
13	CAXVAA	$[Zn_{10}(bbc)_5(bpdc)_2(H_2O)_{10}]NO_3(DEF)_{28}(H_2O)_8$	PCAT + INT (**hcb**)[i]	**hcb**, 3,3,4,5L14, [001]; **bbc**, $Zn_2(COO)_3$	2012, 153
14	PAQCOZ	$[Ag(cpba)_2]SbF_6$	ICAT of INT-2f[j]	**sql**, [1$\bar{1}$0] and [110], Ag	1998, 154
15	REBBUX	$[Zn_2(L^1)(H_2O)]\cdot NO_3\cdot DMF$	ICAT of INT-2f[k]	**hcb**, [100] and [010], L^1 and $Zn_2(COO)_3$	2012, 155

[a]Abbreviations for ligands: bphy =1,2-bis(4-pyridyl)hydrazine; bpp = 4,4′-propane-1,3-diyldipyridine 1,3-bis(4-pyridyl)propane; cpba = 3-cyanophenyl 4-cyanobenzoate; pyada = *N*,*N*′-di(4-pyridyl)adipoamide; tcphb = 1,3,5-tris(4-cyanophenoxymethyl)-2,4,6-trimethylbenzene; tipa = tris(4-imidazolylphenyl)amine; tppt = 2,4,6-tris[4-(pyridin-4-ylthio)methyl]phenyl-1,3,5-triazine; 1,3-bix = 1,3-bis(imidazol-1-ylmethyl) benzene; 1,4-bpeb = 1,4-bis[2-(4-pyridyl)ethenyl]benzene; Hpeba = 3-[2-(4-pyridyl)ethenyl]benzoic acid; H_2bpdc = biphenyl-4,4′-dicarboxylic acid; H_2mfda = 9,9-dimethylfluorene-2,7-dicarboxylic acid; H_2nbpdc = 2,2′-dinitro-4,4′-biphenyldicarboxyl acid; H_2nip = 5-nitroisophthalic acid; H_2pda = phenylenediacrylic acid; H_2tp = terephthalic acid; H_3bbc = 4,4′,4″-[benzene-1,3,5-triyl-tris(benzene-4,1-diyl)]tribenzoate; H_3L^1= 4′,4″,4‴-[(2,4,6-trimethylbenzene-1,3,5-triyl)tris(methyleneoxy)]tribiphenyl-4-carboxylic acid; DMF = dimethylformamide; DMSO = dimethyl sulfoxide. [b]INT-*n*f = *n*-fold interpenetrated [c]Stacking sequence ABCABC. [d]Stacking sequence ABAB. [e]Doc = 3 (1 + 1 + 1); Is = 2. [f]Doc = 5 (2 + 2 + 1); Is = 2. [g]Doc = 8 (3 + 3 + 2); Is = 3. [h]Doc = 10 (2 + 2 + 2 + 2 + 2); Is = 6. [i]**2hcb** + 3,3,4,5L14 with Doc = 2 and Is = 1. [j]Angle 83.5°, view down [001]; Doc = 3/3. [k]Angle 90°, view down [001]; Doc = 5/5.

presence of different types of entanglement of the layers (see Table 3).

An extreme situation consists of the presence of both single and interpenetrated 2D layers simultaneously. Three of these species (FAGCAS and FAGCEW[143] and VAMXEO01[144]) show the stacking of alternate single and 2-fold interpenetrated layers. Interestingly, [Zn(tp)(bphy)] (VAMXEO)[156] was also isolated without clathrate solvents and consists of the same 2-fold layers as VAMXEO01[144] but without intercalation of single ones, the difference arising from the conditions and ratio of reactants used in the solvothermal synthesis. On the other hand, in ACUCAC[142] we observe two distinct single layers intercalating into the stacked 2-fold interpenetrated layers (see Figure 34).

Other species (XOFYUM[157] and OWUFOC[158]) containing polymeric 1D motifs intercalated within 2-fold interpenetrated layers have been omitted here and considered only from the point of view of the interpenetration phenomenon.

The most populated group (eight entries) consists of *n*-fold interpenetrated layers that are further polycatenated in a parallel fashion to give the overall 3D structure (PCAT of 2-fold or 3-fold interpenetrated layers). Here we observe both interpenetration and parallel polycatenation of 2D layers, that is, two distinct types of entanglement in the same species.[159] The *n*-fold interpenetrated motifs (2-fold in six cases and 3-fold in two cases) are characterized by the coplanarity of the involved layers (that share the same average plane, as discussed above). These are further catenated with the adjacent (upper and lower) identical (parallel but offset) interpenetrated motifs to give the 3D array.

The entanglements here discussed contain individual motifs that are either markedly undulated single layers or thick double layers. It is interesting to compare the 2-fold interpenetrated species (see Figure 35). There are two distinct groups depending

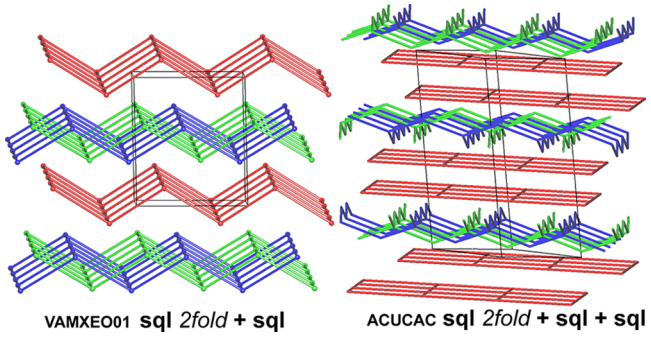

Figure 34. Entanglements with the presence of both single and interpenetrated 2D layers simultaneously.

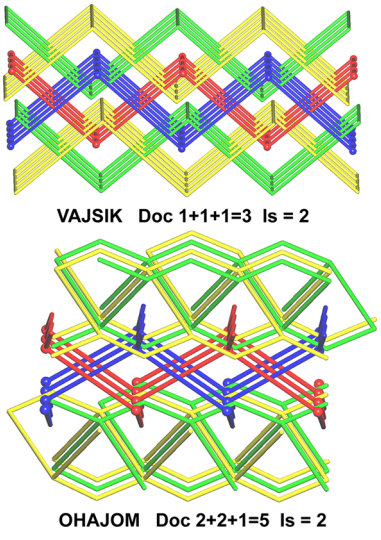

Figure 35. Parallel polycatenation of 2-fold interpenetrated layers.

dx.doi.org/10.1021/cr500150m | *Chem. Rev.* 2014, 114, 7557−7580

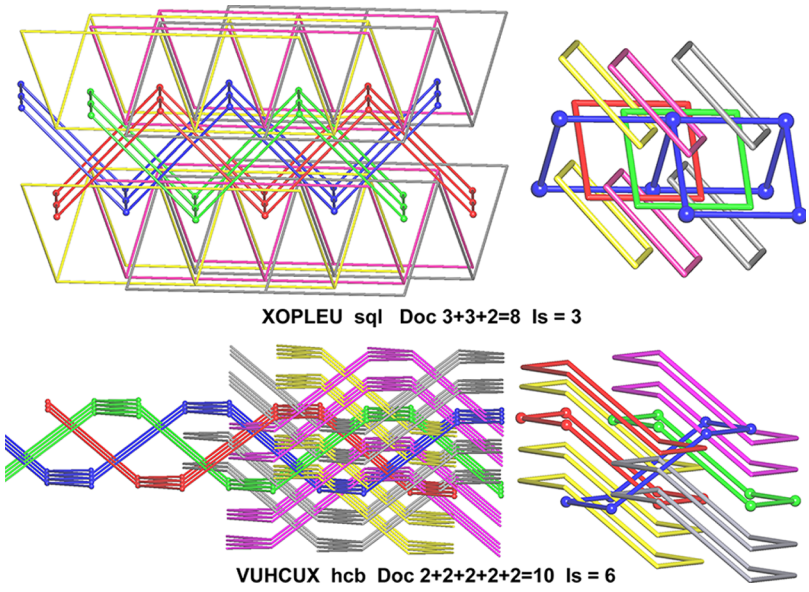

Figure 36. Parallel polycatenation of 3-fold interpenetrated layers.

on the way in which the interpenetrated layers are stacked, leading to different values of the degree of catenation (Doc). In **hcb** ISABUZ[145] and **sql** VAJSIK,[146] all the undulated layers stack, maintaining the same direction of the running waves (stacking nearly in a AAAA sequence), and the same happens for the thick layer 3,4L127 in WAPCIB.[147] It turns out that each individual layer is catenated to only one motif of the upper 2-fold layer and one of the lower 2-fold layer in addition to that interpenetrated in the same plane (1 + 1 + 1), giving Doc = 3. On the other hand, in **sql** MATJIC,[149] **sql** OHAYOM,[150] and the thick layer 3,3L20 KAXTUA,[148] upon passing from an interpenetrated layer to the upper and lower adjacent ones, the waves change drastically their running direction (i.e., the stacking sequence is ABAB). As a consequence, each individual layer is catenated to all the motifs of the upper and lower 2-fold layers in addition to that interpenetrated in the same plane (2 + 2 + 1), giving Doc = 5.

The two examples of polycatenation (XOPLEU[151] and VUHCUX[152]) of 3-fold interpenetrated layers are more complicated. In XOPLEU, the 3-fold interpenetrated layers stack in an ABAB sequence (see Figure 36). This implies that each individual layer is catenated to all three motifs of the upper and lower interpenetrated layers in addition to two in the same plane (3 + 3 + 2). It was correctly observed that each square window of one motif is catenated to six rings only: two belonging to two motifs in the upper layer, two belonging to two motifs in the lower layer, and two in the same plane. Nonetheless, the value of Doc is 8, as stated above. The two statements, however, are not conflicting since the catenation of one motif with an adjacent (upper or lower) motif involves only $^{2}/_{3}$ of the rings. In the case of VUHCUX, the 3-fold interpenetrated layers show a different stacking when compared with XOPLEU, that is, of the AAAA type (see Figure 36). Each individual motif is catenated to two of the three motifs of the upper and lower interpenetrated layers in addition to two in the same plane. Moreover, as correctly described by the authors, the 3-fold interpenetrated layers are interlocked not only with the two nearest-neighboring layers but also with the second-nearest-neighboring layers (see Figure 36). Therefore, the overall polycatenation motif is (2 + 2 + 2 + 2 + 2); that is, the Doc value is 10.

A unique case of mixed entanglement is that of CAXVAA.[153] In this species we have a rare simultaneous occurrence of both polycatenation (involving honeycomb triple layers 3,3,4,5L14 with Doc = 2 and Is = 1) and interpenetration of four **hcb** layers for each of the triple ones, as shown in Figure 37.

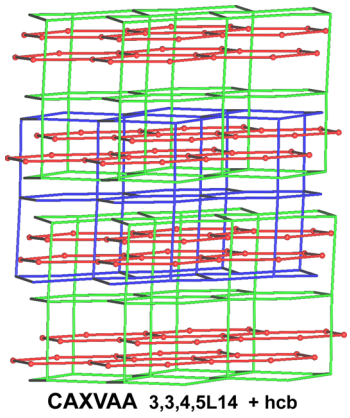

Figure 37. Unique example of parallel polycatenation of thick layers (blue and green) with interpenetration of single **hcb** (red).

The simultaneous existence of interpenetration and inclined polycatenation is a quite rare event, and a unique structure has been known for many years since 1998 (PAQCOZ).[154] Only in 2012 was the second case reported (REBBUX).[155] In both species, two sets of 2D 2-fold interpenetrated layers of **sql** and **hcb** topology, respectively, are interlaced in an inclined fashion. The difference in the entanglements consists mainly of the fact that in PAQCOZ each square ring is catenated with three rings of three other layers (1 + 1 + 1), giving Doc = 3/3, while in REBBUX each **hcb** ring is catenated with five rings of five other layers (1 + 2 + 2), giving Doc = 5/5 (see Figure 38) . In the former species a ring is catenated with one inclined 2-fold interpenetrated layer, while in the latter species it is catenated with two such interpenetrated layers.

Finally, we must briefly mention in this section the case of Ag_2[1,2-bis(4-pyridyl)ethane]$_2$(4,4′-biphenyldicarboxylate) (WUJDIO[80]) that is included in the group of parallel

dx.doi.org/10.1021/cr500150m | *Chem. Rev.* 2014, 114, 7557−7580

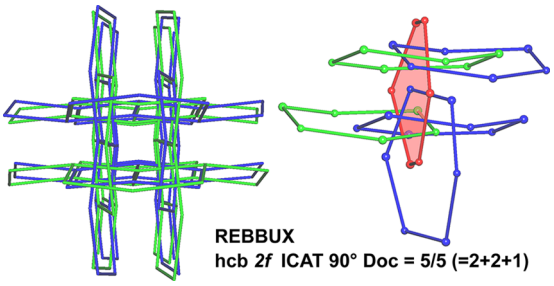

Figure 38. Inclined polycatenation of 2-fold interpenetrated **hcb** layers. On the right the catenation of one 6-ring (in red) with five rings from five different layers shows the origin of Doc 5/5 from 5 = 2 + 2 + 1.

polycatenated frameworks. It was previously discussed in great detail for its unusual and puzzling topological features.[2c] The structure is composed of two distinct sets of parallel polycatenated 2D bilayers of (8^2.10)-KIa topology that appear inextricably entangled. However, each individual 2D motif is interlocked only by the two nearest-neighboring ones of the same set and, quite surprisingly, no motifs of one set are catenated (via Hopf links) by individual motifs of the other set (see Figure 39).

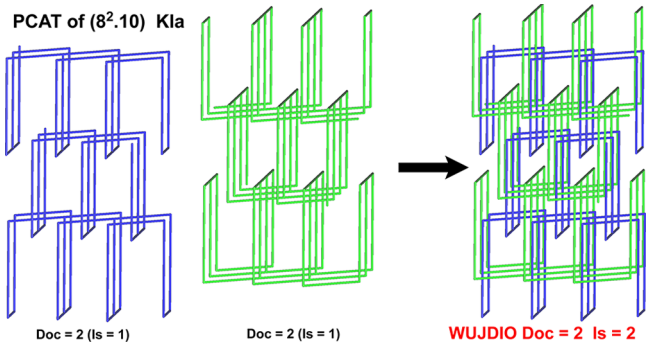

Figure 39. Parallel polycatenation of two sets of KIa layers observed in WUJDIO.

Each polycatenated set has Doc = 2 and Is = 1, while the whole array has Doc = 2 and Is = 2. The exact nature of the linkage between the two sets of layers still awaits a correct topological classification. Certainly the catenation of the rings of one set prevents the disentanglement of the other set and vice versa. The situation is ideally comparable to that of a recently reported exceptional species formed by polycatenation of 0D metal–organic adamantane-like cages, producing a 2-fold interpenetrated 3D **pcu** network: here the 0D motifs are catenated only with other ones of the same 3D net, but their catenation does not allow the disentanglement of the entire architecture.[2f,160]

4. CONCLUSIONS

The investigation of entangled two-dimensional frameworks has shown that this is a numerous family including 783 cases (CSD, version 5.34, November 2012). The entangled phenomena account for about 10% of the total 2D sample, while interpenetration in 3D structures accounts for about 17%.

In spite of this decrease, the species discussed here are particularly intriguing because of the richness of the 2D net topology and the variety of observed types of entanglement. In addition to the well-established phenomena of interpenetration (the dominant one), polycatenation (parallel and inclined), and Borromean linked systems, other classes exhibiting puzzling topologies have been observed and discussed. Thus, we have envisaged the possibility of a new type of entanglement, intermediate between interpenetration and parallel polycatenation, that is composed of a finite number of layers catenated in a parallel fashion (*n*-catenanes), with only a few cases presently known. A separate section has been devoted to the detailed analysis of entangled layers containing 2-node loops threaded by edges of adjacent layers (43 examples). Within Borromean linked systems, in addition to the well-known examples of Borromean 2D waves or Borromean 3D frames, we describe a few exceptional cases of *n*-fold Borromean (non-Brunnian) layers with *n* = 5 and 7. We have also systematically classified for the first time all the cases exhibiting different types of entanglement in the same structure.

Finally, from the point of view of properties and potential applications, these entangled 2D motifs show behavior that can be essentially considered typical of dynamic/flexible porous frameworks (soft porous materials) that can respond to external stimuli of various types by changing their porosity. This leads to guest-induced transformations, solid-state reactions, breathing behavior, selective molecular recognition, and different magnetic properties. Interestingly, of the different types of entanglement, polycatenated species (parallel and inclined) seem the more promising.

Though some of these rare types of entanglement may now appear somewhat exotic, we believe that other examples of such unusual systems will be observed in the near future and that a rationalization of their complexity can be a useful contribution to the engineering of coordination polymers and metal–organic frameworks and their properties, considering the explosive growth of this area in recent years.

ASSOCIATED CONTENT

Supporting Information

References and classification for all 783 structures examined (xls); one table, listing the distribution of network topologies among PCAT entanglement, and three figures, showing 17 thick layers already observed nonentangled, VUKHEP in two possible representations, and a single **kgd** observed in 2-fold interpenetrated TONFUY (pdf). This material is available free of charge via the Internet at http://pubs.acs.org.

AUTHOR INFORMATION

Corresponding Authors

*E-mail lucia.carlucci@unimi.it.
*E-mail davide.proserpio@unimi.it.
*E-mail blatov@samsu.ru.

Notes

The authors declare no competing financial interest.

dx.doi.org/10.1021/cr500150m | *Chem. Rev.* 2014, 114, 7557–7580

Biographies

Lucia Carlucci was born in Italy in 1963. She obtained the "Laurea" degree in Industrial Chemistry (1989) and a Ph.D. in Chemical Sciences (1993) from the University of Bologna. She moved to the University of Milan in 1993. Since 2010 she has been Associate Professor of General and Inorganic Chemistry at the Department of Chemistry of the same university. After early interests in organometallic chemistry, her research activity was oriented to porous coordination polymers and focused on the development of new designed ligands and synthetic strategies, X-ray diffraction, and topological and entanglement analyses.

Gianfranco Ciani was born in Ferrara (Italy) in 1944. He retired from academic activity in 2010 after being Full Professor of Inorganic Chemistry at the University of Milano and Director of DCSSI. Since 1969 in Milano, his activity was devoted to X-ray crystallographic studies of coordination and organometallic compounds, mainly carbonyl metal clusters. Since 1993 his main interest has been devoted to the study of coordination networks and their topologies and to the crystal engineering of mineralomimetic and nanoporous 2D and 3D networks. He is the author of over 236 publications.

Davide M. Proserpio was born in Italy in 1962. In 1986 he earned the "'Laurea'" degree in Chemistry at the University of Pavia. In the next five years he was active in the field of applied theoretical chemistry under the supervision of Carlo Mealli (CNR, Florence, Italy) and Roald Hoffmann (Cornell University, Ithaca, NY). Since 1991 he has been at the University of Milano, as an Associate Professor from 2003, with special interest in topological crystal chemistry: interpenetration, polycatenation, and polythreading of nets.

Tatyana G. Mitina was born in 1988 in Mednogorsk, Orenburg region, Russia. She graduated from Samara State University in 2010 and now is a researcher at Samara Center for Theoretical Materials Science. Her research interests concern topological analysis of two-periodic coordination polymers and applications of computer methods to the design of new materials.

Vladislav A. Blatov was born in 1965 in Samara (formerly Kuibyshev), Russia. He graduated from Samara State University (1987) and earned degrees of Candidate (1991) and Doctor in Chemistry (1998) from the Institute of General and Inorganic Chemistry (Moscow). He has been a Full Professor in the SSU Chemistry Department since 1998 and

dx.doi.org/10.1021/cr500150m | *Chem. Rev.* 2014, 114, 7557−7580

director of the Samara Center for Theoretical Materials Science since 2013. His research and educational interests concern geometrical and topological methods in crystal chemistry and their computer implementation in the program package TOPOS, being developed since 1989.

ACKNOWLEDGMENTS

D.M.P., T.G.M., and V.A.B. thank the Russian government (Grant 14.B25.31.0005) and the Russian Foundation for Basic Research (Grant 13-07-00001) for support.

REFERENCES

(1) (a) Long, J., Yaghi, O. , Guest Eds. 2009 Metal−Organic Frameworks Issue. *Chem. Soc. Rev.* **2009**, *38* (5). (b) Zhou, H.-C, Long, J., Yaghi, O. , Guest Eds. 2012 Metal−Organic Frameworks Issue. *Chem. Rev.* **2012**, *112*, 673−1268. (c) Batten, S. R.; Neville, S. M.; Turner, D. R. *Coordination Polymers: Design, Analysis and Application*; Royal Society of Chemistry: Cambridge, U.K., 2009. (d) Farrusseng, D. *Metal−Organic Frameworks Applications from Catalysis to Gas Storage*; Wiley: Weinheim, Germany, 2011. (e) *Metal−Organic Frameworks Design and Application*; MacGillivray, L. R., Ed.; Wiley: Hoboken, NJ, 2010. (f) Batten, S. R.; Champness, N. R.; Chen, X.-M.; Garcia-Martinez, J.; Kitagawa, S.; Öhrström, L.; O'Keeffe, M.; Suh, M. P.; Reedijk, J. *Pure Appl. Chem.* **2013**, *85*, 1715.

(2) (a) Batten, S. R.; Robson, R. *Angew. Chem., Int. Ed.* **1998**, *37*, 1460. (b) Batten, S. R. *Curr. Opin. Solid State Mater. Sci.* **2001**, *5*, 107. (c) Carlucci, L.; Ciani, G.; Proserpio, D. M. *Coord. Chem. Rev.* **2003**, *246*, 247. (d) Blatov, V. A.; Carlucci, L.; Ciani, G.; Proserpio, D. M. *CrystEngComm* **2004**, *6*, 377. (e) Carlucci, L.; Ciani, G.; Proserpio, D. M. In *Making Crystals by Design: Methods, Techniques and Applications*; Braga, D., Grepioni, G., Eds.; Wiley−VCH: Weinheim, Germany, 2007; Chapt. 1.3. (f) Proserpio, D. M. *Nat. Chem.* **2010**, *2*, 435. (g) Forgan, R. S.; Sauvage, J.-P.; Stoddart, J. F. *Chem. Rev.* **2011**, *111*, 5434. (h) Delgado-Friedrichs, O.; Foster, M. D.; O'Keeffe, M.; Proserpio, D. M.; Treacy, M. M. J.; Yaghi, O. M. *J. Solid State Chem.* **2005**, *178*, 2533.

(3) Mitina, T. G.; Blatov, V. A. *Cryst. Growth Des.* **2013**, *13*, 1655.

(4) Duchamp, D. J.; Marsh, R. E. *Acta Crystallogr.* **1969**, *B25*, 5.

(5) AGMANI: Konnert, J.; Britton, D. *Inorg. Chem.* **1966**, *5*, 1193.

(6) Furukawa, H.; Cordova, E. K.; O'Keeffe, M.; Yaghi, O. M. *Science* **2013**, *341*, No. 1230444.

(7) Blatov, V. A.; Shevchenko, A. P.; Proserpio, D. M. *Cryst. Growth Des.* **2014**, DOI: 10.1021/cg500498k.

(8) Baburin, I.; Blatov, V. A.; Carlucci, L.; Ciani, G.; Proserpio, D. M. *J. Solid State Chem.* **2005**, *178*, 2452.

(9) Baburin, I. A.; Blatov, V. A.; Carlucci, L.; Ciani, G.; Proserpio, D. M. *Cryst. Growth Des.* **2008**, *8*, 519.

(10) Baburin, I. A.; Blatov, V. A.; Carlucci, L.; Ciani, G.; Proserpio, D. M. *CrystEngComm* **2008**, *10*, 1822.

(11) (a) Foo, M. L.; Matsuda, R.; Kitagawa, S. *Chem. Mater.* **2014**, *26*, 310. (b) Horike, S.; Shimomura, S.; Kitagawa, S. *Nat. Chem.* **2009**, *1*, 695. (c) Uemura, K.; Matsuda, R.; Kitagawa, S. *Solid State Chem.* **2005**, *178*, 2420. (d) Kitagawa, S.; Uemura, K. *Chem. Soc. Rev.* **2005**, *34*, 109.

(12) Miller, J. S.; Vos, T. E.; Shum, W. W. *Adv. Mater.* **2005**, *17*, 2251.

(13) (a) Jiang, H.-L.; Makal, T. A.; Zhou, H.-C. *Coord. Chem. Rev.* **2013**, *257*, 2232. (b) Yang, G.-P.; Hou, L.; Ma, L.-F.; Wang, Y.-Y. *CrystEngComm* **2013**, *15*, 2561.

(14) Alexandrov, E. V.; Blatov, V. A.; Kochetkov, A. V.; Proserpio, D. M. *CrystEngComm* **2011**, *13*, 3947.

(15) (a) O'Keeffe, M.; Yaghi, O. A. *Chem. Rev.* **2012**, *112*, 675. (b) Li, M.; Li, D.; O'Keeffe, M.; Yaghi, O. A. *Chem. Rev.* **2014**, *114*, 1343.

(16) (a) O'Keeffe, M.; Peskov, M. A.; Ramsden, S. J.; Yaghi, O. M. *Acc. Chem. Res.* **2008**, *41*, 1782. (b) Blatov, V. A.; O'Keeffe, M.; Proserpio, D. M. *CrystEngComm* **2010**, *12*, 44. (c) http://rcsr.anu.edu.au/.

(17) (a) Koch, E.; Fischer, W. *Z. Kristallogr.* **1978**, *148*, 107. (b) Koch, E.; Fischer, W.; Sowa, H. *Acta Crystallogr.* **2006**, *A62*, 152.

(18) TONFUY: Lan, Y.-Q.; Li, S.-L.; Qin, J.-S.; Du, D.-Y.; Wang, X.-L.; Su, Z.-M.; Fu, Q. *Inorg. Chem.* **2008**, *47*, 10600.

(19) Yang, J.; Ma, J.-F.; Batten, S. R. *Chem. Commun.* **2012**, *48*, 7899.

(20) Carlucci, L.; Ciani, G.; Proserpio, D. M. *CrystEngComm.* **2003**, *5*, 269.

(21) Alexandrov, E. V.; Blatov, V. A.; Proserpio, D. M. *Acta Crystallogr.* **2012**, *A68*, 484.

(22) ZABQIC01: Venkataraman, D.; Lee, S.; Moore, J. S.; Zhang, P.; Hirsch, K. A.; Gardner, G. B.; Covey, A. C.; Prentice, C. L. *Chem. Mater.* **1996**, *8*, 2030.

(23) OYEYOH: Wu, H.; Yang, J.; Su, Z.-M.; Batten, S. R.; Ma, J.-F. *J. Am. Chem. Soc.* **2011**, *133*, 11406.

(24) SAYMUB01: Shattock, T. R.; Vishweshwar, P.; Wang, Z.; Zaworotko, M. J. *Cryst. Growth Des.* **2005**, *5*, 2046.

(25) COKPIC, COKPOI, and SOCYEP01: Liu, J.-Q.; Wang, Y.-Y.; Ma, L.-F.; Wen, G.-L.; Shi, Q.-Z.; Batten, S. R.; Proserpio, D. M. *CrystEngComm* **2008**, *10*, 1123.

(26) SOCYEP: Hu, Y.; Li, G.; Liu, X.; Hu, B.; Bi, M.; Gao, L.; Shi, Z.; Feng, S.; Shi, Z.; Feng, S. *CrystEngComm* **2008**, *10*, 888.

(27) FUYWIG and FUYWOM: Chang, Y.; Xu, H.; Xie, S.; Li, J.; Xue, X.; Hou, H. *Inorg. Chem. Commun.* **2010**, *13*, 959.

(28) Delgado Friedrichs, O.; O'Keeffe, M.; Yaghi, O. M. *Solid State Sci.* **2003**, *5*, 73.

(29) UDIROP: Du, M.; Jiang, X.-J.; Zhao, X.-J. *Inorg. Chem.* **2007**, *46*, 3984.

(30) FAMGEH: Hu, J.-S.; Qin, L.; Zhang, M.-D.; Yao, X.-Q.; Li, Y.-Z.; Guo, Z.-J.; Zheng, H.-G.; Xue, Z.-L. *Chem. Commun.* **2012**, *48*, 681.

(31) EWOTAM: Ma, L.-F.; Li, C.-P.; Wang, L.-Y.; Du, M. *Cryst. Growth Des.* **2011**, *11*, 3309.

(32) IXOHOT: Hu, J.; Huang, L.; Yao, X.; Qin, L.; Li, Y.; Guo, Z.; Zheng, H.; Xue, Z. *Inorg. Chem.* **2011**, *50*, 2404.

(33) MULFEE: Hou, H.; Wei, Y.; Song, Y.; Zhu, Y.; Li, L.; Fan, Y. J. *Mater. Chem.* **2002**, *12*, 838.

(34) REDSEZ: Gao, E.-Q.; Xu, Y.-X.; Cheng, A.-L.; He, M.-Y.; Yan, C.-H. *Inorg. Chem. Commun.* **2006**, *9*, 212.

(35) MAVNOO: Liang, W.; Peng, C.; Wenbin, L. *Chem. Commun.* **2012**, *48*, 2846.

(36) NULJOU, NULJOU01, NULJUA: Zhuang, C.-F.; Zhang, J.; Wang, Q.; HuaChu, Z.; Fenske, D.; Su, C.-Y. *Chem.—Eur. J.* **2009**, *15*, 7578.

(37) SAQFOG: Ye, Q.; Li, Y.-H.; Song, Y.-M.; Huang, X.-F.; Xiong, R.-G.; Xue, Z. *Inorg. Chem.* **2005**, *44*, 3618.

(38) BOBGEF and BOBGIJ: Yang, J.; Ma, J.-F.; Batten, S. R.; Su, Z.-M. *Chem. Commun.* **2008**, 2233.

(39) The suggested definition is as follows: a "nontrivial polyrotaxane" is any system with at least one polymeric component where the components cannot be separated without the breaking of links and where the entanglement is such that 2-membered rings of one component are penetrated by rods of another.

(40) ANARIR and ANAROX: Jin, X.-H.; Sun, J.-K.; Cai, L.-X.; Zhang, J. *Chem. Commun.* **2011**, *47*, 2667.

(41) DAYMEX: Liu, J.-Q.; Wu, J.; Wang, Y.-Y.; Ma, D.-Y. *Coord. Chem.* **2012**, *65*, 1303.

(42) DUCFOX, DUCFUD, and DUCHIT: Dong, B.-X.; Xu, Q. *Inorg. Chem.* **2009**, *48*, 5861.

(43) ETEKUK and ETELAR: Chen, H.; Xiao, D.; He, J.; Li, Z.; Zhang, G.; Sun, D.; Yuan, R.; Wang, E.; Luo, Q.-L. *CrystEngComm* **2011**, *13*, 4988.

(44) EVUSEU: Karmakar, A.; Titi, H. M.; Goldberg, I. *Cryst. Growth Des.* **2011**, *11*, 2621.

(45) EYEYIR: Chen, L.; Shao, K.-Z.; Yuan, G.; Yang, G.-S.; Zang, H.-Y.; Xu, G.-J.; Wang, X.-L.; Su, Z.-M. *Z. Anorg. Allg. Chem.* **2011**, *637*, 1414.

(46) GALKIP: Liu, G.-X.; Xu, H.; Zhou, H.; Nishihara, S.; Ren, X.-M. *CrystEngComm* **2012**, *14*, 1856.

(47) GUBZIN, GUBZOT, and GUBZUZ: Dong, B.-X.; Xu, Q. *Cryst. Growth Des.* **2009**, *9*, 2776.

(48) IQEJOE: Liu, Y.-Y.; Wang, Z.-H.; Bo, L.; Liu, Y.-Y.; Ma, J.-F. *CrystEngComm* **2011**, *13*, 3811.

(49) KEZPIP: Zhuang, W.-J.; Sun, C.-Y.; Jin, L.-P. *Polyhedron* **2007**, *26*, 1123.
(50) LALFOV: Xu, H.; Juhasz, G.; Yoshizawa, K.; Takahashi, M.; Kanegawa, S.; Sato, O. *CrystEngComm* **2010**, *12*, 4031.
(51) MARMID: Liu, J.-Q.; Wang, Y.-Y.; Wu, T.; Wu, J. *CrystEngComm* **2012**, *14*, 2906.
(52) MUNPIV and MUNPUH: Liu, Y.; Qi, Y.; Lv, Y.-Y.; Che, Y.-X.; Zheng, J.-M. *Cryst. Growth Des.* **2009**, *9*, 4797.
(53) NEBSUI: Hoskins, B. F.; Robson, R.; Slizys, D. A. *Angew. Chem., Int. Ed.* **1997**, *36*, 2336.
(54) NUDDAS, NUDDEW, and NUDDIA: Cao, X.-Y.; Yao, Y.-G.; Batten, S. R.; Ma, E.; Qin, Y.-Y.; Zhang, J.; Zhang, R.-B.; Cheng, J.-K. *CrystEngComm* **2009**, *11*, 1030.
(55) OVIDAZ: Zhang, Y.-N.; Liu, P.; Wang, Y.-Y.; Wu, L.-Y.; Pang, L.-Y.; Shi, Q.-Z. *Cryst. Growth Des.* **2011**, *11*, 1531.
(56) QUQGOZ: Ma, Y.; Cheng, A.-L.; Gao, E.-Q. *Cryst. Growth Des.* **2010**, *10*, 2832.
(57) RUBGIF: Wang, J.; Zhang, Y.; Ji, Y. *Solid State Sci.* **2009**, *11*, 364.
(58) SULKEQ: Li, N.; Chen, L.; Lian, F.-Y.; Jiang, F.-L.; Hong, M.-C. *Jiegou Huaxue (Chin. J. Struct. Chem.)* **2009**, *28*, 1417.
(59) TAHNIB: Liu, G.-X.; Xu, Y.-Y.; Wang, Y.; Nishihara, S.; Ren, X.-M. *Inorg. Chim. Acta* **2010**, *363*, 3932.
(60) TONFIM, TONFOS, and TONGAF: Lan, Y.-Q.; Li, S.-L.; Qin, J.-S.; Du, D.-Y.; Wang, X.-L.; Su, Z.-M.; Fu, Q. *Inorg. Chem.* **2008**, *47*, 10600.
(61) UYOHOG: Liu, G.-X.; Cha, X.-C.; Li, X.-L.; Zhang, C.-Y.; Wang, Y.; Nishihara, S.; Ren, X.-M. *Inorg. Chem. Commun.* **2011**, *14*, 867.
(62) UZAWEY: Liu, H.-W.; Lu, W.-G. *Wuji Huaxue Xuebao (Chin. J. Inorg. Chem.)* **2011**, *27*, 1810.
(63) WOCKOP: Wang, G.-H.; Li, Z.-G.; Jia, H.-Q.; Hu, N.-H.; Xu, J.-W. *Cryst. Growth Des.* **2008**, *8*, 1932.
(64) WODGUS: Luo, F.; Yang, Y.-T.; Che, Y.-X.; Zheng, M. *CrystEngComm* **2008**, *10*, 981.
(65) YOCPEL: Goodgame, D. M. L.; Menzer, S.; Smith, A. M.; Williams, D. J. *Angew. Chem., Int. Ed.* **1995**, *34*, 574.
(66) WAGXAF and WAGXEJ: Zhang, Z.-H.; Chen, S.-C.; Mi, J.-L.; He, M.-Y.; Chen, Q.; Du, M. *Chem. Commun.* **2010**, *46*, 8427.
(67) UHUROF: Liu, J.-Q.; Wang, Y.-Y.; Liu, P.; Dong, Z.; Shi, Q.-Z.; Batten, S. R. *CrystEngComm* **2009**, *11*, 1207.
(68) CUXTIZ: Chen, L.; Xu, G.-J.; Shao, K.-Z.; Zhao, Y.-H.; Yang, G.-S.; Lan, Y.-Q.; Wang, X.-L.; Xu, H.-B.; Su, Z.-M. *CrystEngComm* **2010**, *12*, 2157.
(69) Yerin, A.; Wilks, E. S.; Moss, G. P.; Harada, A. *Pure Appl. Chem.* **2008**, *80*, 2041.
(70) In ref 19 this species has been considered as a case of "nontrivial polyrotaxane", of type IVb, since it does fulfill all the criteria proposed for this type of entanglement, according to the definition given.[38] Nevertheless, the presence of Hopf links involving the shortest circuits of the nets seems to us a good reason to prefer a classification like parallel polycatenation.
(71) WUVBUK: Zhang, X.-M.; Chen, X.-M. *Eur. J. Inorg. Chem.* **2003**, 413.
(72) MEBBIE: Carlucci, L.; Ciani, G.; Proserpio, D. M.; Rizzato, S. *Chem. Commun.* **2000**, 1319.
(73) LOTQUG: Batten, S. R.; Harris, A. R.; Jensen, P.; Murray, K. S.; Ziebell, A. *J. Chem. Soc., Dalton Trans.* **2000**, 3829.
(74) NORDAZ: Liu, F.-Q.; Tilley, T. D. *Inorg. Chem.* **1997**, *36*, 5090.
(75) XODJOQ: Li, M.-X.; Miao, Z.-X.; Shao, M.; Liang, S.-W.; Zhu, S.-R. *Inorg. Chem.* **2008**, *47*, 4481.
(76) BOQSEG: Ashiry, K. O.; Zhao, Y.-H.; Shao, K.-Z.; Su, Z.-M.; Xu, G.-J. *Polyhedron* **2009**, *28*, 975.
(77) BURGAX: Han, Z.-B.; Zhang, G.-X. *CrystEngComm* **2010**, *12*, 348.
(78) OKEJIY: Qin, L.; Hu, J.-S.; Huang, L.-F.; Li, Y.-Z.; Guo, Z.-J.; Zheng, H.-G. *Cryst. Growth Des.* **2010**, *10*, 4176.
(79) WAVTEU: Zhao, X.; Dou, J.; Sun, D.; Cui, P.; Sun, D.; Wu, Q. *Dalton Trans.* **2012**, *41*, 1928.
(80) WUJDIO: Fu, Z.-Y.; Wu, X.-T.; Dai, J.-C.; Hu, S.-M.; Du, W.-X. *New J. Chem.* **2002**, *26*, 978.
(81) Zhao, X.; Liu, F.; Zhang, L.; Sun, D.; Wang, R.; Ju, Z.; Yuan, D.; Sun, D. *Chem.—Eur. J.* **2014**, *20*, 649.
(82) (a) Li, D.; Kaneko, K. *Chem. Phys. Lett.* **2001**, *335*, 50. (b) Cheng, Y.; Kondo, A.; Noguchi, H.; Kajiro, H.; Urita, K.; Ohba, T.; Kaneko, K.; Kanoh, H. *Langmuir.* **2009**, *25*, 4510.
(83) Kondo, A.; Noguchi, H.; Ohnishi, S.; Kajiro, H.; Tohdoh, A.; Hattori, Y.; Xu, W. C.; Tanaka, H.; Kanoh, H.; Kaneko, K. *Nano Lett.* **2006**, *6*, 2581.
(84) Fletcher, A. J.; Cussen, E. J.; Prior, T. J.; Rosseinsky, M. J.; Kepert, C. J.; Thomas, K. M. *J. Am. Chem. Soc.* **2001**, *123*, 10001.
(85) Kajiro, H.; Kondo, A.; Kaneko, K.; Kanoh, H. *Int. J. Mol. Sci.* **2010**, *11*, 3803.
(86) (a) XAFCUE, XAFDAL, XAFDEP, XAFDIT, XAFDOZ, and XAFDUF: Aijaz, A.; Lama, P.; Bharadwaj, P. K. *Eur. J. Inorg. Chem.* **2010**, 3829. (b) VULWEF: Higuchi, M.; Tanaka, D.; Horike, S.; Sakamoto, H.; Nakamura, K.; Takashima, Y.; Hijikata, Y.; Yanai, N.; Jungeun, K. I. M.; Kato, K.; Kubota, Y.; Takata, M.; Kitagawa, S. *J. Am. Chem. Soc.* **2009**, *131*, 10336.
(87) WAVVIA: Gong, Y.; Qin, J. B.; Wu, T.; Li, J.-H.; Yang, L.; Cao, R. *Dalton Trans.* **2012**, *41*, 1961.
(88) JITHUQ, JITJAY, JITJEC, and JITJIG: Lin, J.-G.; Su, Y.; Tian, Z.-F.; Qiu, L.; Wen, L.-L.; Lu, Z.-D.; Li, Y.-Z.; Meng, Q.-J. *Cryst. Growth Des.* **2007**, *7*, 2526.
(89) Zaworotko, M. J. *Chem. Commun.* **2001**, 1.
(90) EHOVON: Zhao, L.-M.; Zhai, B.; Gao, D.-L.; Shi, W.; Zhao, B.; Cheng, P. *Inorg. Chem. Commun.* **2010**, *13*, 1014.
(91) MAHYID: Carlucci, L.; Ciani, G.; Proserpio, D. M. *New J. Chem.* **1998**, *22*, 1319.
(92) GIMGEP: Tian, Z.; Lin, J.; Su, Y.; Wen, L.; Liu, Y.; Zhu, H.; Meng, Q.-J. *Cryst. Growth Des.* **2007**, *7*, 1863.
(93) MOVSEW: Cao, X.-Y.; Lin, Q.-P.; Qin, Y.-Y.; Zhang, J.; Li, Z.-J.; Cheng, J.-K.; Yao, Y.-G. *Cryst. Growth Des.* **2009**, *9*, 20.
(94) SARFOH: Zeng, M.-H.; Zhang, W.-X.; Sun, X.-Z.; Chen, X.-M. *Angew. Chem., Int. Ed.* **2005**, *44*, 3079.
(95) VIRYIF: Qi, Y.-F.; Xiao, D.; Wang, E.; Zhang, Z.; Wang, X. *Aust. J. Chem.* **2007**, *70*, 871.
(96) MUPZON: Hulvey, Z.; Furman, J. D.; Turner, S. A.; Tang, M.; Cheetham, A. K. *Cryst. Growth Des.* **2010**, *10*, 2041.
(97) EWAXUV: Carlucci, L.; Ciani, G.; Proserpio, D. M.; Spadacini, L. *CrystEngComm* **2004**, *6*, 96.
(98) KOLPEH: Liu, G.-X.; Zhu, K.; Chen, H.; Huang, R.-Y.; Ren, X.-M. *CrystEngComm* **2008**, *10*, 1527.
(99) EJAXOC: Carlucci, L.; Ciani, G.; Proserpio, D. M.; Rizzato, S. *CrystEngComm* **2003**, *5*, 190.
(100) VUXXOC: Wang, S.; Wang, D.; Dou, J.; Li, D. *Acta Crystallogr.* **2010**, *C66*, m141.
(101) QOVYEF: Moliner, N.; Munoz, C.; Letard, S.; Solans, X.; Menendez, N.; Goujon, A.; Varret, F.; Real, J. A. *Inorg. Chem.* **2000**, *39*, 5390.
(102) REBWUQ: Kondo, M.; Shimamura, M.; Noro, S.; Minakoshi, S.; Asami, A.; Seki, K.; Kitagawa, S. *Chem. Mater.* **2000**, *12*, 1288.
(103) OTUYAE: Gong, Y.; Li, J.; Qin, J. B.; Wu, T.; Cao, R.; Li, J. H. *Cryst. Growth Des.* **2011**, *11*, 1662.
(104) NIMQOQ: Pike, R. D.; de Krafft, K. E.; Ley, A. N.; Tronic, T. A. *Chem. Commun.* **2007**, 3732.
(105) BIYFAR: Wang, Y.-H.; Li, Y.-W.; Chen, W.-L.; Li, Y.-G.; Wang, E.-B. *J. Mol. Struct.* **2008**, *877*, 56.
(106) GIDMUC: Chen, S.-M.; Zhang, J.; Lu, C.-Z. *CrystEngComm* **2007**, *9*, 390.
(107) (a) GUTDOO, GUTDOO01, and GUTDUU: Halder, G. J.; Kepert, C. J.; Moubaraki, B.; Murray, K. S.; Cashion, J. D. *Science* **2002**, *298*, 1762. (b) CEZDAN, CEZDAN01, and CIDGEC: Neville, S. M.; Moubaraki, B.; Murray, K. S.; Kepert, C. J. *Angew. Chem., Int. Ed.* **2007**, *46*, 2059. (c) YOBZAR, YOBYUK and YOBYUK01: Neville, S. M.; Halder, G. J.; Chapman, K. W.; Duriska, M. B.; Southon, P. D.; Cashion, J. D.; Letard, J.-F.; Moubaraki, B.; Murray, K. S.; Kepert, C. J. *J. Am. Chem. Soc.* **2008**, *130*, 2869. (d) DORCIX01, DORCIX02, and DORCIX03: Halder, G. J.; Chapman, K. W.; Neville, S. M.; Moubaraki, B.; Murray, K. S.; Letard, J.-F.; Kepert, C. J. *J. Am. Chem. Soc.* **2008**, *130*,

17552. (e) OHOSEK, OHOSIO, OHOSOU01, and OHOSUA01: Neville, S. M.; Halder, G. J.; Chapman, K. W.; Duriska, M. B.; Moubaraki, M.; Murray, K. S.; Kepert, C. J. *J. Am. Chem. Soc.* **2009**, *131*, 12106.
(108) UNEGEA: Xu, B.; Lin, X.; He, Z.; Lin, Z.; Cao, R. *Chem. Commun.* **2011**, *47*, 3766.
(109) (a) ILUXOD and ILUXIX: Polunin, R. A.; Kolotilov, S. V.; Kiskin, M. A.; Cador, O.; Mikhalyova, E. A.; Lytvynenko, A. S.; Golhen, S.; Ouah, L.; Ovcharenko, V. I.; Eremenko, I. L.; Novotortsev, V. M.; Pavlishchuk, V. V. *Eur. J. Inorg. Chem.* **2010**, 5055. (b) Polunin, R. A.; Kolotilov, S. V.; Kiskin, M. A.; Cador, O.; Golhen, S.; Shvets, O. V.; Ouahab, L.; Dobrokhotova, Z. V.; Ovcharenko, V. I.; Eremenko, I. L.; Novotortsev, V. M.; Pavlishchuk, V. V. *Eur. J. Inorg. Chem.* **2011**, 4985. (c) AQOSOP: Wang, S.; Li, L.; Zhang, J.; Yuan, X.; Su, C.-Y. *Mater. Chem.* **2011**, *21*, 7098.
(110) (a) UZIZOT: Poong, J. I.; Koo, H. G.; Pak, H. M.; Jang, S. P.; Lee, Y. J.; Kim, C.; Kim, S.-J.; Kim, Y. *Inorg. Chim. Acta* **2011**, *376*, 605. (b) KUPFEH and KUPFIL: Miao, X.-H.; Zhu, L.-G. *Dalton Trans.* **2010**, *39*, 1457.
(111) AKAXIU, AKAXOA, AKAXUG, AKAYAN, AKAYER: Yang, R.; Li, L.; Xiong, Y.; Li, J.-R.; Zhou, H.-C.; Su, C.-Y. *Chem.—Asian J.* **2010**, *5*, 2358.
(112) Chichak, K. S.; Cantrill, S. J.; Pease, A. R.; Chiu, S. H.; Cave, G.W. V.; Atwood, J. L.; Stoddart, J. F. *Science* **2004**, *304*, 1308.
(113) (a) Liantonio, R.; Metrangolo, P.; Meyer, F.; Pilati, T.; Navarrini, W.; Resnati, G. *Chem. Commun.* **2006**, 1819. (b) Men, Y.-B.; Sun, J.; Huang, Z.-T.; Zheng, Q.-Y. *Angew. Chem., Int. Ed.* **2009**, *48*, 2873. (c) Jang, J.-J.; Li, L.; Yang, T.; Kuang, D.-B.; Wang, W.; Su, C.-Y. *Chem. Commun.* **2009**, 2387.
(114) DAPPAN: Jiang, L.; Meng, X.-R.; Xiang, H.; Ju, P.; Zhong, D.-C.; Lu, T.-B. *Inorg. Chem.* **2012**, *51*, 1874.
(115) GUWXIF: Suh, M. P.; Choi, H. J.; So, S. M.; Kim, B. M. *Inorg. Chem.* **2003**, *42*, 676.
(116) ICIWOG: Leznoff, D. B.; Xue, B.-Y.; Batchelor, R. J.; Einstein, F. W. B.; Patrick, B. O. *Inorg. Chem.* **2001**, *40*, 6026.
(117) IWENII: Xu, C.; Guo, Q.; Wang, X.; Hou, H.; Fan, Y. *Cryst. Growth Des.* **2011**, *11*, 1869.
(118) LIKBIR: Li, J.; Song, L.; Du, S. *Inorg. Chem. Commun.* **2007**, *10*, 358.
(119) NEQDET: Dobrzanska, L.; Lloyd, G. O.; Jacobs, T.; Rootman, I.; Oliver, C. L.; Bredenkamp, M. W.; Barbour, L. *J. Mol. Struct.* **2006**, *796*, 107.
(120) PUNRUM: Adarsh, N. N.; Dastidar, P. *Cryst. Growth Des.* **2010**, *10*, 483.
(121) RESHUT: Lu, X.-Q.; Pan, M.; He, J.-R.; Cai, Y.-P.; Kang, B.-S.; Su, C.-Y. *CrystEngComm* **2006**, *8*, 827.
(122) SAVCAU: Dobrzanska, L.; Raubenheimer, H. G.; Barbour, L. J. *Chem. Commun.* **2005**, 5050.
(123) TANJEZ: Zhang, J.; Xue, Y.-S.; Li, Y.-Z.; Du, H.-B.; You, X.-Z. *CrystEngComm* **2011**, *13*, 2578.
(124) WOCXIW and WOCXOC: Byrne, P.; Lloyd, G. O.; Clarke, N.; Steed, J. W. *Angew. Chem., Int. Ed.* **2008**, *47*, 5761.
(125) MUHVOB and MUHVOB01: Jiang, Y.-Y.; Ren, S.-K.; Ma, J.-P.; Liu, Q.-K.; Dong, Y.-B. *Chem.—Eur. J.* **2009**, *15*, 10742.
(126) YUXGOO and YUXGUU: Burrows, A. D.; Frost, C. G.; Mahon, M. F.; Raithby, P. R.; Richardson, C.; Stevenson, A. J. *Chem. Commun.* **2010**, *46*, 5064.
(127) AHIDEA: Muthu, S.; Yip, J. H. K.; Vittal, J. *J. Chem. Soc., Dalton Trans.* **2002**, 4561.
(128) HOFXOP and HOFXUV: Tong, M.-L.; Chen, X.-M.; Ye, B.-H.; Ji, L.-N. *Angew. Chem., Int. Ed.* **1999**, *38*, 2237.
(129) KAVDAN, KAVDER, and KAVDIV: Sun, Y.-Q.; Zhang, J.; Ju, Z.-F.; Yang, G.-Y. *Cryst. Growth Des.* **2005**, *5*, 1939.
(130) UZAZUR: Chen, J.-X.; Lin, W.-E.; Zhou, C.-Q.; Yau, L. F.; Wang, J.-R.; Wang, B.; Chen, W.-H.; Jiang, Z.-H. *Inorg. Chim. Acta* **2011**, *376*, 389.
(131) WIYMIA: Lee, E.; Heo, J.; Kim, K. *Angew. Chem., Int. Ed.* **2000**, *39*, 2699.
(132) YANWOB, YANWUH, YANXAO, and YANXAO01: Sun, J.-K.; Yao, Q.-X.; Tian, Y.-Y.; Wu, L.; Zhu, G.-S.; Chen, R.-P.; Zhang, J. *Chem.—Eur. J.* **2012**, *18*, 1924.
(133) GIQGAP and GIQGET: Zhang, X.-L.; Guo, C.-P.; Yang, Q.-Y.; Wang, W.; Liu, W.-S.; Kang, B.-S.; Su, C.-Y. *Chem. Commun.* **2007**, 4242.
(134) ISAROK: Burrows, A. D.; Kelly, D. J.; Mahon, M. F.; Raithby, P. R.; Richardson, C.; Stevenson, A. J. *Dalton Trans.* **2011**, *40*, 5483.
(135) Liang, C.; Mislow, K. *J. Math. Chem.* **1994**, *16*, 27.
(136) (a) Baas, N. A.; Seeman, N. C. *J. Math. Chem.* **2012**, *50*, 220. (b) Baas, N. A. *Int. J. Gen. Syst.* **2013**, *42*, 137.
(137) DOJFUD: Zavalii, P. Y.; Olijnik, V. V.; Mys'kiv, M. G.; Chikhrii, S. I.; Zavalii, A. Y. *Crystallogr. Rep.* **1985**, *30*, 1081.
(138) UGUGAF: Yao, Q.-X.; Jin, X.-H.; Ju, Z.-F.; Zhang, H.-X.; Zhan, J. *CrystEngComm.* **2009**, *11*, 1502.
(139) FUWVUP: Shi, X.; Wang, W.; Hou, H.; Fan, Y. *Eur. J. Inorg. Chem.* **2010**, 3652.
(140) For some recent attempts, see (a) Evans, M. E. Ph.D. Thesis, Australian National University, 2011; https://digitalcollections.anu.edu.au/handle/1885/9502. (b) Evans, M. E.; Robins, V.; Hyde, S. T. *Acta Crystallogr.* **2013**, *A69*, 241.
(141) FUYBUX: Men, Y.-B.; Sun, J.; Huang, Z.-T.; Zheng, Q.-Y. *Chem. Commun.* **2010**, *46*, 6299.
(142) ACUCAC: Evans, O. R.; Lin, W. *Chem. Mater.* **2001**, *13*, 3009.
(143) FAGCAS and FAGCEW: Carlucci, L.; Ciani, G.; Proserpio, D. M.; Rizzato, S. *CrystEngComm* **2002**, *4*, 121.
(144) VAMXEO01: Liu, X.-M.; Lin, R.-B.; Zhang, J.-P.; Chen, X.-M. *Inorg. Chem.* **2012**, *51*, 5686.
(145) ISABUZ: Banfi, S.; Carlucci, L.; Caruso, E.; Ciani, G.; Proserpio, D. M. *Cryst. Growth Des.* **2004**, *4*, 29.
(146) VAJSIK: Liu, D.; Li, H.-X.; Liu, L.-L.; Wang, H.-M.; Li, N.-Y.; Ren, Z.-G.; Lang, J.-P. *CrystEngComm* **2010**, *12*, 3708.
(147) WAPCIB: Li, B.; Yang, F.; Zhang, Y.; Li, G.; Zhou, Q.; Hua, J.; Shi, Z.; Feng, S. *Dalton Trans.* **2012**, *41*, 2677.
(148) KAXTUA: Wu, H.; Yang, J.; Liu, Y.-Y.; Ma, J.-F. *Cryst. Growth Des.* **2012**, *12*, 2272.
(149) MATJIC: Xu, X.; Zhang, X.; Liu, X.; Wang, L.; Wang, E. *CrystEngComm* **2012**, *14*, 3264.
(150) OHAYOM: Guo, H.; Qiu, D.; Guo, X.; Batten, S. R.; Zhang, H. *CrystEngComm* **2009**, *11*, 2611.
(151) XOPLEU: Hsu, Y.-F.; Hu, H.-L.; Wu, C.-J.; Yeh, C.-W.; Proserpio, D. M.; Chen, J.-D. *CrystEngComm* **2009**, *11*, 168.
(152) VUHCUX: Yang, Q.-Y.; Zheng, S.-R.; Yang, R.; Pan, P.; Cao, R.; Su, C.-Y. *CrystEngComm* **2009**, *11*, 680.
(153) CAXVAA: Hauptvogel, I. M.; Bon, V.; Grunker, R.; Baburin, I. A.; Senkovska, I.; Mueller, U.; Kaskel, S. *Dalton Trans.* **2012**, *41*, 4172.
(154) PAQCOZ: Hirsch, K. A.; Wilson, S. R.; Moore, J. S. *Chem. Commun.* **1998**, 13.
(155) REBBUX: Chen, L.; Tan, K.; Lan, Y.-Q. *Chem. Commun.* **2012**, *48*, 5919.
(156) VAMXEO: Wang, H.; Szeto, L.; Chan, W. T. K.; Yeung, H.-L.; Wong, K.-L.; Wong, W.-T. *Can. J. Chem.* **2012**, *90*, 100.
(157) XOFYUM: Ayyappan, P.; Evans, O. R.; Lin, W. *Inorg. Chem.* **2002**, *41*, 3328.
(158) OWUFOC: Tian, L.; Zhang, Z.-J.; Yu, A.; Shi, W.; Chen, Z.; Cheng, P. *Cryst. Growth Des.* **2010**, *10*, 3847.
(159) Polycatenation of interpenetrated layers (sharing the same average plane), was previously observed in an exceptional organic array (POVJAL) sustained by hydrogen bonds and derived by the self-assembly of 1,1,1-tris(4-hydroxyphenyl)ethane and 4,4′-bipyridyl, to give a 2:3 adduct. The **hcb** puckered 2D nets give parallel (2D → 2D) 5-fold interpenetrated sheets that are polycatenated into a unique 3D array. Each layer is interlinked with 10 others, that is, four sharing the same average plane, plus three of the five "above" and three of the five "below" (Doc = 10). Benyei, A. C.; Coupar, P. I.; Ferguson, G.; Glidewell, C.; Longh, A. J.; Meehan, P. R. *Acta Crystallogr.* **1998**, *C54*, 1515.
(160) Kuang, X.; Wu, X.; Yu, R.; Donahue, J. P.; Huang, J.; Lu, C.-Z. *Nat. Chem.* **2010**, *2*, 461.